Parametric Investigation of Thick Metallic Section (Aerospace Alloys) Cutting by Abrasive Water Jet

By:

Lubna Sharif

Registration Number: **00000204365**

Session**: 2017-21**

Supervised by:

Professor Dr. Khalid Mahmood

A Thesis Submitted to Department of Mechanical Engineering for Advance Study in Machining in Partial Fulfilment of the Requirements for the Degree of Master of Science in Mechanical Engineering

Mechanical Engineering Department

College of Electrical & Mechanical Engineering (CEME)

National University of Sciences and Technology,

Rawalpindi

September 2021

Parametric Investigation of Thick Metallic Section (Aerospace Alloys) Cutting by Abrasive Water Jet

Author

Lubna Sharif

Registration Number: **00000204365**

A Thesis Submitted in Partial Fulfilment of the Requirements for the Degree of Master of Science in Mechanical Engineering

Thesis Supervisor:

Professor Dr. Khalid Mahmood

Thesis Supervisor's Signature:

MECHANICAL ENGINEERING DEPARTMENT

COLLEGE OF ELECTRICAL & MECHANICAL ENGINEERING (CEME)

NATIONAL UNIVERSITY OF SCIENCES AND TECHNOLOGY, RAWALPINDI

SEPTEMBER 2021

Thesis Acceptance Certificate

Certified that final copy of MS/ MPhil thesis written by Ms Lubna Sharif (Registration No: 00000204365), of College of Electrical & Mechanical Engineering (School/ College/ Institute) has been vetted by undersigned, found complete is all respects as per NUST Statutes/ Regulations, is free of plagiarism, errors and mistakes and is accepted as partial fulfilment for award of MS/ MPhil Degree. It is further certified that necessary amendments as pointed out by GEC members of the scholar have also been incorporated in the said thesis.

Signature: _____

Supervisor: Dr. Khalid Mahmood

Date: _____

Signature: _____

Head of Department: Dr Imran Akhtar

Date: _____

Signature: _____

Dean: Dr Aamer Baqai

Date: _____

FORM TH-4

National University of Science and Technology

MASTER THESIS WORK

We hereby recommend that the dissertation prepared under our supervision by **Lubna Sharif** (00000204365) titled: *"***Parametric Investigation of Thick Metallic Section (Aerospace Alloys) Cutting by Abrasive Water Jet**" be accepted in partial fulfilment of the requirements for the MS Mechanical Engineering Degree with (___) grade.

Examination Committee Members

1. Brig Dr. Syed Waheed Ul Haq Signatures: _____

2. Dr. Bilal Anjum Signatures: _____

Supervisor: Dr. Khalid Mahmood Signatures: _____

Date: _____

Head of Department: Dr Imran Akhtar Signatures: _____

Date: _____

COUNTERSIGNED

Dean: Dr Aamer Baqai Signatures: _____

Date: _____

Declaration

I certified that this research work titled *"***Parametric Investigation of Thick Metallic Section (Aerospace Alloys) Cutting by Abrasive Water Jet**" is my own work. The work has not been presented elsewhere for assessment. The material that has been used from other sources has been properly acknowledge/ referred.

Ms Lubna Sharif

(00000204365)

Proposed Certificate for Plagiarism

It is certified that MS Thesis Titled *"***Parametric Investigation of Thick Metallic Section (Aerospace Alloys) Cutting by Abrasive Water Jet**" by **Ms Lubna Sharif (00000204365)** has been examined by us.
We undertake the follows:

a. Thesis has significant new work/knowledge as compared already published or are under consideration to be published elsewhere. No sentence, equation, diagram, table, paragraph or section has been copied verbatim from previous work unless it is placed under quotation marks and duly referenced.

b. The work presented is original and own work of the author (i.e. there is no plagiarism). No ideas, processes, results or words of others have been presented as Author own work.

c. There is no fabrication of data or results which have been compiled/ analyzed.

d. There is no falsification by manipulating research materials, equipment or processes, or changing or omitting data or results such that the research is not accurately represented in the research record.

e. The thesis has been checked using TURNITIN (copy of original report attached) and found within limits as per HEC plagiarism policy and instructions issued from time to time.

Supervisor: _____

Dr. Khalid Mahmood

Copyright Statement

Acknowledgement

Today, I stand humbled, indebted, and obligated to my MS Supervisor Dr. Khalid Mahmood, without whose support and guidance this work would have never been possible. In the process, I kept bothering him and he very graciously clarified all my doubts without showing an iota of annoyance. His prompt reply to emails, text messages made my hard task easy-going.

I also owe profound acknowledgment to my GEC members, Brigadier Dr. Syed Waheed ul Haq and Dr. Bilal Anjum for offering their all-out support and guidance at every step of my project. The list of supporting staff is long enough but I would like to make mention of my co-student Engineer Shahid Hussain, lab staff for their untiring dedication.

I would definitely like to make a mention of Heavy Industries Taxila, for giving me an opportunity to work on Abrasive Water Jet Machines out of their busy schedule and People's Steel Mills (Pvt) Ltd for providing me Inconel 600 on gratis basis for this project.

I would like to pay special gratitude to my great mother who always encouraged me to dream big and my husband who was always present to support me during thick and thin. During this long MS tenure, my daughters learned to cook themselves rather than bothering me. A hot cup of coffee or tea at my study table helped me burn my midnight oil for which my son also deserves acknowledgement. Last but not least I would like to thank my brother, my class fellows, senior and junior students who were always ready to help me at every step.

Today I stand proud but humbled in front of Allah Almighty for He is the only praiseworthy.

Dedication

This thesis is lovingly dedicated to my loving parents for their unconditional love all the years for which I am short of suitable words, with special mention of my mentor; my mother, who has always been a source of motivation for me to pursue my dreams

&

my husband who has a plenty of shares in pursuit of my obsession

&

my respected teachers, who acted as a beacon to my curiosity in quest for knowledge and wisdom.

Abstract

Titanium and nickel alloys exhibit exceptional mechanical and physical properties which make them suitable for being used in the aerospace industry. Since these are classified as hard-to-cut materials, hence they are machined using conventional methods leads to several issues such as work hardening, tool blending and surface defects. These issues can be resolved by selecting non-conventional machining methods. This study aims at machining titanium grade V and Inconel 600 using the fastest developing Abrasive Water Jet (AWJ) technique. An optical microscope, surface profilometer, and scanning electron microscopy (SEM) were utilized to examine the quality of the machined surface, microstructural features, and grain distortion. To discover major process parameters that affect statistically the surface roughness and kerf angle, the Taguchi technique, and analysis of variance (ANOVA) were used. Results revealed traverse speed as the most important factor affecting kerf angle for both alloys. However, traverse speed and water pressure showed significant influence on surface roughness of Inconel 600 and Titanium grade V, respectively. Embedment of abrasive particles was analysed using energy dispersive spectroscopy (EDS), X-ray diffraction (XRD) and scanning electron microscopy (SEM) analysis.

Keywords: Abrasive water jet, aerospace alloys, kerf angle, surface roughness, grain distortion,

Table of Contents

	Page
Abstract……	x
List of Figure..……..	xiii
List of Table…….....	xv
Nomenclature……	xvii
Chapter 1: "Introduction"	
1.1 Background……	1
1.2 Thesis Design……..	1
1.3 Problem Statement……..	2
1.4 Research Objectives……	2
Chapter 2: "Literature Review"	
2.1 Aerospace Alloys……	3
2.1.1 Titanium Alloys (Properties and Conventional Cutting Problems)…….	3
2.1.2 Nickel Alloys (Properties and Conventional Cutting Problems)…….	4
2.2 Abrasive Water Jet Machining……	5
2.2.1 Introduction of Abrasive Water Jet……..	5
2.2.2 Working Principle of Abrasive Water Jet……	5
2.2.3 Main Components and Working……..	6
2.2.4 Abrasive Used……..	7
2.2.5 Advantages of Abrasive Water Jet……	7
2.2.6 Applications of Abrasive Water Jet…….	8
2.2.7 AWJM Process Parameters……	9
2.3 Literature Review……	9
2.4 Flow Chart for Experimentation…….	13
2.5 Summary of Chapter 2……	14
CHAPTER 3: "Experimentation"	
3.1 List of Equipment……...	15
3.2 Work Piece Material……...	15
3.3 EDS Analysis……	15
3.4 Mechanical Properties……...	17
3.5 Abrasive Water Jet Machine…….	18
3.6 Abrasive Used……..	19
3.7 Selection of Process Parameters…….	20
3.8 Design of Experiment……	22
3.9 Methodology……..	22
3.10 Measurements of Response Parameters……...	23
3.11 Taguchi Methodology……..	25
3.12 SEM Analysis……...	26
3.13 XRD Analysis……...	28
3.14 Summary of Chapter…….	29
Chapter 4: "Abrasive Water jet Cutting of Inconel 600"	
4.1 Introduction…….	30
4.2 Kerf Angle Results…….	30
4.3 Ker Angle Analysis…….	33

4.4 Optimal Process Parameters (KA)…… 34
4.5 Surface Roughness Results…… 35
4.6 Surface Roughness Analysis…… 37
4.7 Optimal Process Parameters (SR)…… 38
4.8 Analysis for Abrasive Entrapment (XRD + SEM)…… 39
4.9 Grain Distortion Measurement (SEM)…… 41
4.10 Summary of Chapter…… 42
CHAPTER 5: "Abrasive Water Jet Cutting of Titanium Grade V"
5.1 Introduction…… 43
5.2 Kerf Angle Results…… 43
5.3 Kerf Angle Analysis…… 46
5.4 Optimal Process Parameters (KA)…… 47
5.5 Surface Roughness Results…… 48
5.6 Surface Roughness Analysis…… 50
5.7 Optimal Process Parameters (SR)…… 51
5.8 Analysis for Abrasive Entrapment (XRD)…… 52
5.9 Grain Distortion Measurement (SEM)…… 53
5.10 Summary of Chapter…… 55
CHAPTER 6: "Conclusions"
6.1 Introduction…… 56
6.2 Conclusions for Inconel 600…… 56
6.3) Conclusions for Titanium Grade V…… 57
6.4) Recommendations…… 57
References..... 58

List of Figures

Page

Figure 1.1 Layout for thesis design…….. 1

Figure 2.1 Turbofan engine of Rolls Royce…… 3

Figure 2.2 Components of AWJ Machine…… 6

Figure 2.3 Cutting head of AWJ machine…… 7

Figure 2.4 Flow chart for experimentation……... 13

Figure 3.1 EDS spectrum of Inconel 600……. 16

Figure 3.2 SEM image during composition test……... 16

Figure 3.3 EDS spectrum of Titanium grade V…… 17

Figure 3.4 SEM image during composition test……... 17

Figure 3.5 Abrasive water jet machine……. 18

Figure 3.6 EDS spectrum of garnet…….. 19

Figure 3.7 EDS image during composition test…… 19

Figure 3.8 SEM image for particle size…… 20

Figure 3.9 Sample after AWJ machining……. 23

Figure 3.10 AWJM cut……..... 24

Figure 3.11 Image from optical microscope……. 24

Figure 3.12 Surface roughness profile of sample I-1/4…… 25

Figure 3.13 Machined sample before mounting……... 26

Figure 3.14 Mounted sample…… 27

Figure 4.1 Data means plot for kerf angle…… 32

Figure 4.2 Data means plot for surface roughness……... 37

Figure 4.3 XRD pattern for Inconel 600…….. 40

Figure 4.4 SEM image of machined sample…… 40

Figure 4.5 Grain distortion of machined surface……. 42

Figure 5.1 Data means plot for kerf angle…… 45

Figure 5.2 Data means plot for surface roughness……... 50

Figure 5.3 XRD pattern of Titanium grade V…….. 52

Figure 5.4 Zoomed XRD pattern of Titanium grade V…… 53

Figure 5.5 Grain distortion of machined surface…….. 54

List of Tables

Page

Table 2.1 Process parameters influencing AWJ machining process……... 9

Table 3.1 Comparison of material composition Inconel 600……... 16

Table 3.10 Machine setting for polishing of mounted samples……... 28

Table 3.2 Comparison of material composition Titanium grade V……. 16

Table 3.3 Hardness results for Inconel 600 & Titanium grade V…… 17

Table 3.4 AWJ machine specification…….. 18

Table 3.5 Comparison of material composition abrasive garnet…….. 19

Table 3.6 Processes parameter and their levels…… 21

Table 3.7 Experimental plan using an L9 orthogonal array……. 22

Table 3.8 Experimental Conditions for AWJM……... 23

Table 3.9 Machine setting for grinding mounted samples……... 28

Table 4.1 Results of kerf angle……. 30

Table 4.10 Optimal process parameters for surface roughness…… 38

Table 4.11 Chemical composition of AWJ machined sample……. 40

Table 4.12 Grain distortion of AWJ machined samples…….. 41

Table 4.2 Response table for mean kerf angle……. 31

Table 4.3 Variance analysis for kerf angle……... 31

Table 4.4 Model summary for kerf angle……. 32

Table 4.5 Optimal process parameters for kerf angle…….. 34

Table 4.6 Results for surface roughness……... 35

Table 4.7 Response table for mean surface roughness……. 35

Table 4.8 Variance analysis for surface roughness…….. 36

Table 4.9 Model summary for surface roughness…… 36

Table 5.1 Results for kerf angle……... 43

Table 5.10 Optimal process parameters for surface roughness…… 51

Table 5.11 Grain distortion of AWJ machined samples…….. 54

Table 5.2 Response table for mean kerf angle……. 44

Table 5.3 Variance analysis for kerf angle……... 44

Table 5.4 Model summary for kerf angle……. 45

Table 5.5 Optimal process parameters for kerf angle…….. 47

Table 5.6 Results for surface roughness……... 48

Table 5.7 Response table for mean surface roughness……. 48

Table 5.8 Variance analysis for surface roughness…….. 49

Table 5.9 Model summary for surface roughness…… 49

Nomenclature

AWJM Abrasive water jet machining

AFR Abrasive flow rate

DOE Design of experiments

EDS Energy dispersive analysis

gm/min Grams per minute

KA Kerf angle

LBM Laser beam method

mm Millimetres

mm/min Millimetres per minute

MPa Mega pascal

RPM Revolutions per minute

SR Surface roughness

SEM Scanning electron microscopy

SOD Standoff distance

TS Traverse

WP Water pressure

WEDM Wire electric discharge machine

XRD Xray diffraction

Chapter 1: “Introduction”

1.1) Background

In the world of technological advancement, advanced machining processes are taking over the role of traditional methods. This phenomenon is more pronounced when it comes to cutting hard materials with complex shapes and features. Due to high heat generation, machined surfaces are liable to certain defects with few machining methods. During the cutting process, the inbuilt properties of the target material should not be varied to get desired results. Surface quality, material removal, tool cost, energy applied, and operating time should be kept in mind while the selection of appropriate machining process, otherwise it may initiate many issues which include poor surface, tool blending, work hardening, poor surface finish, other surface issues and certainly higher production cost. Conventional machining processes often come across such issues. It is for this reason that advanced non-conventional processes machining is in high demand. On the contrary, non-conventional machining methods offer great prospects since these process are not susceptible to the target material. Abrasive Water jet (AWJ) and Wire Electric Discharge Machining (WEDM) are examples of such non-conventional machining processes.

1.2) Thesis Design

The Figure 1.1 shown below represents the complete analytical procedure of my research. The design shows the methodology which I have adopted during my thesis

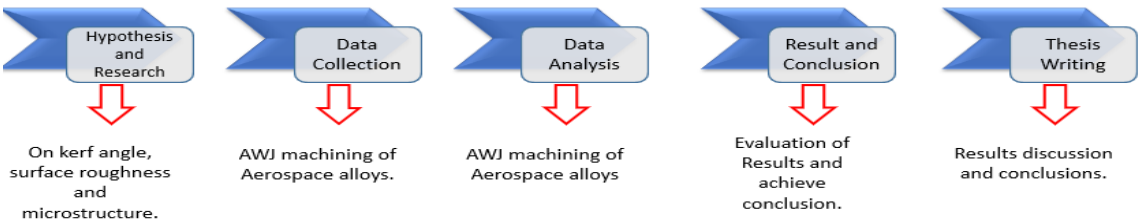

Figure 1.1 Layout for Thesis design

1.3) Problem Statement

Alloys of titanium and nickel are scrutinized as problematic to machine materials using conventional methods because of the work hardening, poor thermal conductivity and rapid deterioration of tool at high cutting temperatures which leads to lower material removal rate and higher production cost. Some non-conventional machining methods for example electric discharge machining and laser machining are also not suitable due to larger heat affected zone and surface quality. One of the fast-growing, non-conventional is abrasive water jet with various advantages e.g., negligible heat affected zone, less cutting forces, and flexibility of materials etc. This study aims at machining titanium and nickel alloys using the AWJ cutting method which has not been amply covered earlier. Furthermore, in most cases, the surface integrity of machined samples was analysed in comparison with other conventional and non-conventional cutting methods whereas, this study intends to cover grain distortion measurement of samples machined at various input parameters using the AWJ technique.

1.4) Research Objectives

The objectives of research work are as follows

- Analyze the influence of cutting variables on kerf angle
- Analyze the influence of cutting variables on surface roughness
- Finding best machine variables for kerf angle and surface roughness
- Evaluation of grain distortion using SEM analysis
- Analyze the abrasive particle entrapment using XRD and EDS analysis

Chapter 2: “Literature Review”

2.1) AEROSPACE ALLOYS

Taking advantage [1] of greater physical and mechanical properties in relation to exceptional corrosion resistance, lasting fatigue, outstanding mechanical strength, and high strength to weight ratio of aerospace materials, therefore, in the recent past, it is preferred to use titanium and nickel alloys over structural steel material. Fig 2.1 reveals a conventional turbofan engine with main sections and the use of fundamental materials. It is quite evident that titanium and nickel-based alloys take a considerable share in the engineering of turbine discs, fan blades and pressure compressors.

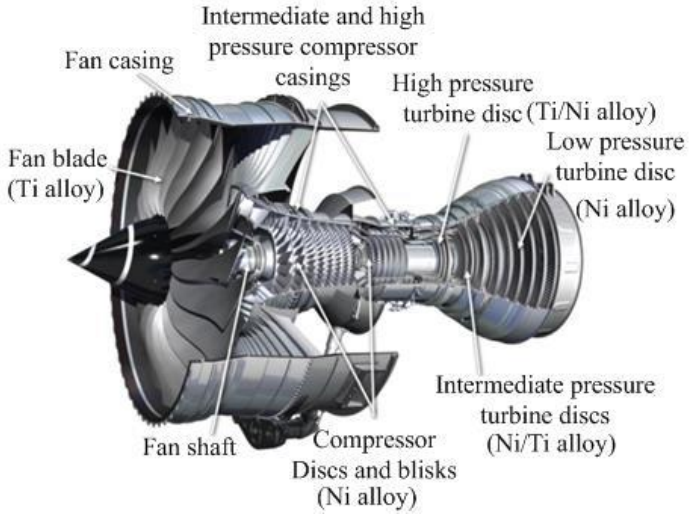

Fig 2.1 Turbofan engine of Rolls Royce showing main parts comprising titanium and nickel alloys

2.1.1) Titanium Alloys

Properties

Owing to the properties [2] like being highly corrosion-resistant, great strength to weight ratio, biocompatibility, and being lightweight titanium as well as its alloys are mostly utilized in aerospace, marine, and medical industries. Titanium grade v is most widely used among various titanium alloys which are widely consumed in the production of aircraft compressors and blades of turbine.

Conventional Cutting Problems

Conventional machining of titanium as well as its alloys is complicated due to certain inherent properties.

- Thermal conductivity lower values results in the accumulation of heat which lowers the life span of the cutting tool.
- A higher value of hardness and strength requires higher cutting forces.
- Titanium being chemical reactive at elevated temperatures with other materials causes a chemical reaction between chip and tool resulting in reduced fatigue strength and tool wear.
- Lower values of elastic modulus cause poor machinability due to the chattering of the workpiece.

2.1.2) Nickel Alloys

Properties

Nickel alloys are [1] highly corrosion and thermal resistant materials. The ability of nickel alloys which makes them a perfect material for utilising aerospace engine's hot section elements is that they maintain their chemical along with mechanical properties at high temperature, which can be ambient temperature up to 600º C. Statistical study/ analysis reveals that roundabout half of an aerospace engine by weight has been produced on an industrial scale by employing nickel alloys.

Conventional Cutting Problems

In the wake of poor machinability, nickel alloys are believed to be hard-to-cut materials that are challenging to process using traditional methods.

- The machining tool easily gets worn out and therefore, the life of the tool declines, which ultimately results in poor surface integrity.
- Since these materials can keep their higher strength combined with hardness at high cutting temperature, therefore warrants higher values of cutting forces.
- Lower value of thermal conductivity of these alloys results in heat accumulation at tool/ target material during the machining process. As a result of thermos-mechanical stresses brought in by cutting temperature gradients and high cutting force, alterations in microstructure and mechanical properties is obvious besides machined surface damage.

Even some non-traditional methods of cutting including laser machining (LM) and electrical discharge machining (EDM) are also not effective methods due to heat affected zone and surface quality.

2.2) Abrasive Water Jet Machine

2.2.1) Introduction

Concept of abrasive jet cutting [3] to replace traditional machine shops was explored by water jet pioneer Dr John Olsen in the early 1990s. His mission was to replace the traditional system with a noiseless and dust-free system. He also eyed on gaining the expertise that was needed by Abrasive Jet in that era. That process is widely cost-effective, and the rate of removal of material is much on a higher side in contrast to traditional machining methods. The abrasive water jet technology comes as an emerging new technology that could handle the cutting of almost all types of materials and profiles in a non-conventional way.

2.2.2) Working Principle

Using a jet of elevated pressure and high-speed water and abrasive mixture in order to remove the material through erosion is the basic principle of abrasive water jet machining technology. It also refers to as conversion of kinetic energy into pressure energy while the target material experiences high stresses. As the induced stress surpasses the material's ultimate shear stress, it starts chipping off and gets loosened to expose a new and fresh surface.

2.2.3) Main Components and Working

A conventional illustration of an abrasive water jet machine is displayed in Fig 2.2

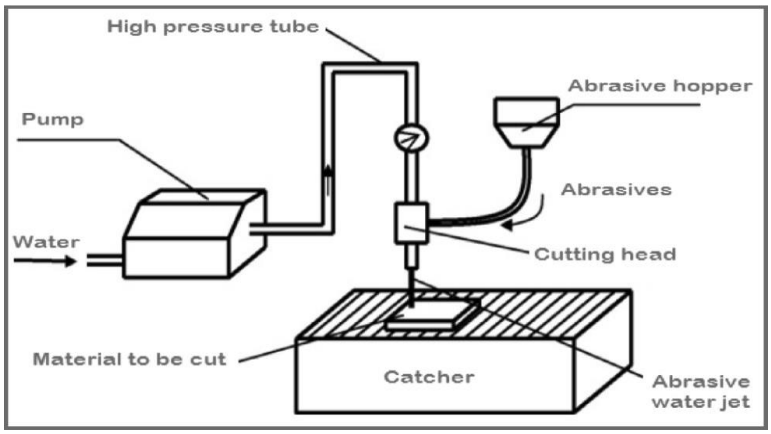

Fig 2.2 Components of AWJ Machine

Major components of Abrasive Water Jet are: -

High-Pressure Generating System

The high-pressure generating system includes an intensifier and an accumulator, which aid in the production of high pressure and the sequential storage of high-pressure water. The intensifier performs as an amplifier, transferring energy from low-pressure hydraulic fluid to ultrahigh-pressure water.

CNC Unit

In machining, high dimensional accuracy is obtained through the CNC unit which regulates the motion of the cutting jet.

Cutting Head

The cutting head as shown in Fig 2.3 comes with a nozzle, orifice, focusing tube, and mixing chamber. A stainless-steel focusing tube is 76.2 mm long with a diameter of 0.76 mm while an orifice with diameter range of 0.08 mm to 0.8 mm and may have sapphire, ruby, and diamond material. Pressured water is transported from the accumulator to the cutting head by means of a focusing tube. Pressure energy of water is converted into kinetic energy of water particles after passing through orifice. When high-pressure water passes through it Venture effect creates a vacuum when water drops its pressure energy while it travels through the mixing chamber. As a result of this vacuum, abrasive particles enter in mixing chamber and join the water. In the mixing chamber, energy is

transferred to abrasive particles and then a mixture of water and abrasive pass-through nozzle with high speed this process is more like a cutting of material by saw.

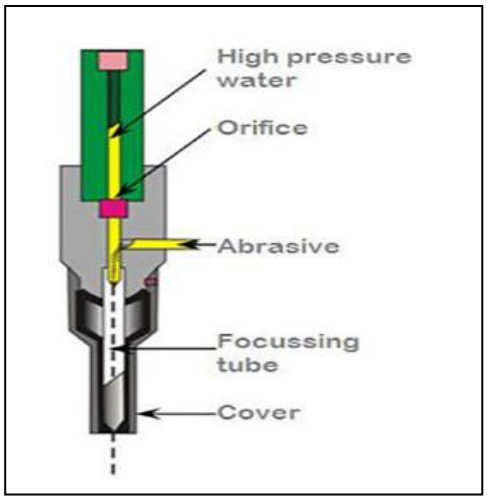

Fig 2.3 Cutting Head of AWJ machine

Catcher

The catcher collects the pressurized water after cutting of material.

2.2.4) Abrasive Used

Garnet (mesh #80) [4] being most effective in giving good cutting depth, is believed to be the most used abrasive. They are of the group of silicate minerals that ensue often in the environment, therefore, are cost-effective.

2.2.5) Advantages of Abrasive Waterjet Machining

Abrasive Water Jet Machining has emerged as a fast-growing non-traditional cutting technology with several advantages [5] over other non-traditional cutting methods.

1) **Flexibility of Material Selection**

   Waterjet is believed to be the most adaptable technique that can cut any material for instance aluminium, ceramics, wood, steel, plastics, stone, laminates and glass etc No limitations are applicable in relation to current conductivity and reflection of light as in the case of WEDM and laser cutting respectively.

2) **Friendly to Environment**

Another attribute of this technology is its environmentally friendly property, in which water and abrasive (most commonly natural material garnet) both can be use again after initial use [6]. It is also free of hazardous fumes, unlike plasma or cutting beams.

3) **Unlimited Thickness**

The water jet technique is useful for cutting both thick and thin material alike while other methods can cut up to a defined thickness only.

4) **No Thermal deformation**

A significant merit of water jet machining is negligible thermal deformation of the material which is being cut. At the cutting arena, a small amount of heat is generated, which is removed due to the continuous water flow resulting in a preserved structure.

5) **Quality of Cut Surface**

Water jet machining presents a very high-quality structure of the cut surface. Therefore, the final product is free from rough edges with no burr formation. As a result, it reduces the extra time, efforts and use of additional machines for giving final finishing to the product.

6) **Compressive Residual Stresses**

This technique yields the most desirable compressive residual stress state in the target section.

2.2.6) Applications of Abrasive Waterjet Machining

In the present era, the use of abrasive water jet technology is being commonly applied in the modern industry which includes but is not limited to construction engineering, chemical process engineering, construction engineering, automotive industry, aerospace industry and environmental technology. Moreover, this technology is also being used in the leather /textile industry, cutting of frozen meat, removal of paint, surgery, and cutting of pocket milling during drilling.

2.2.7) AWJM PROCESS PARAMETERS

The material removal procedure [3] because of contact between the target material and abrasive water jet is firmly governed by several parameters which can be categorised as parameters of input and output. The course of action of abrasive waterjet machining is dealt by many process parameters shown in Table 2.1, which qualify the cost of budget, efficacy, and quality of the complete process.

Table 2.1

Process parameters affecting AWJ machining process

Input Parameters	**Output Parameters**
Water pressure	Surface roughness, striation formation
Traverse speed, no of passes	Kerf angle, top and bottom width
Abrasive flow rate, size, shape, and hardness	Depth of cut
Impact angle	Material removal rate
Standoff distance	
Nozzle diameter, length	
Orifice diameter	

2.3 Literature Review

Titanium and nickel-based alloys are material of choice in many applications. Their high corrosion resistance, high strength and low density makes them more suitable for submarine and aerospace applications. These alloys exhibit excellent bio compatibility and can be used for prosthetic applications like orthopedic implants. However, these alloys are difficult to machine with conventional machining process due to their low thermal conductivity and high reactivity, leading to high cutting temperature and permanent tool failure[1] .

In year 2014 Adnan Akkurt [7] carried out an evaluation of pure and aluminium alloy material which was machined with wire electric discharge machining, abrasive water jet, saw, submerged plasma, oxyfuel, plasma and milling. In this study microstructures and hardness variation of samples machined with various techniques, were investigated. It was found that target material hardness, microstructure and surface finish get affected by the technique of cutting and other than AWJ cutting, microstructural changes were

observed in all cutting methods. AWJ technique was found suitable for industrial usage where microstructural changes and reduction in hardness should not be involved.

In 2018 Jonas Holmberg & Johan Berglund [8] carried out a comparison of surface integrity for non-traditional and traditional machining technique including laser beam machining, abrasive water jet machining. wire electrical discharge machining and milling. The conclusion of this study reflected that AWJM remained best in terms of surface integrity characteristics with compressed leftover stresses in the machined area and a lower surface roughness. In addition to this it was also brought out that low level of residual stresses which are tensile in nature, in the surface with greater surface roughness in EDM and LBM has much negative impact therefore, not recommended as a substitute.

In 2005 examination of impact of orifice and nozzle diameter variance on the capability of AWJ for cutting aluminium alloy was undertaken by John Rozario Jegaraj [9]. The capability was judged with various factors to include removal rate of material, kerf geometry, topography of machined surface and cutting depth. It was found that finishing and efficacy through AWJ could be managed with orifice diameter ranging from 0.25-0.3 mm with maintaining focussing nozzle size up to 1.2mm.

In 2017 Andrzej [4] carried out a study on AWJ cutting of grade V, titanium alloy (Ti6Al4V) with the help of olivine, garnet and crushed glass which revealed that the use of garnet gave the best cutting depth with minor wear factor for focusing tube. It is further revealed that at slower traverse speed, depth of cut was increased.

In the year 2007 Ahmet Hascalik and Ulas Caydas [10] explored the machined surface of Titanium alloy in relation to traverse speed. Machined surfaces of target material were examined by using scanning electron microscopy (SEM) and surface profilometry. Microstructural assessment of the machined surface of samples discovered three different zones:

1) The jet upward deflection zone is called a rough cutting region (RCR)
2) Cutting zone at lower attack angles called an initial damage region (IDR)
3) Cutting zone at large attack angles called a smooth cutting region (SCR)

The final experimental results revealed that the jet's traversal speed is an important factor in surface morphology, and that it is directly related to the sizes and characteristics of various zones created in the cutting facet. Furthermore, in some situations, the kerf ratio and surface roughness were found to be strongly related to traverse speed.

In 2014 [11] analysis for taper angle and surface roughness on aluminium 6351 T6 material was carried out by Mayur C. Patel and Mr S.B. Patel. This methodology was based on the Full Factorial technique, variance analysis (ANOVA) and Regression Analysis to enhance the procedural parameters for efficacious machining. ANOVA was executed to get substantial factors driving Taper Angle in addition to Surface Roughness. In this study, abrasive flow rate and their ratio of ratio are realised to be important factors.

A study conducted by P. Shanmughasundaram [12] in 2014 for A1- graphite composites to analyse the impact of standoff distance, water pressure and traverse speed on the surface roughness using L9 Taguchi technique. It was established that the water pressure was the prime machining factor following this, were traverse speed and the standoff distance respectively. Further examination revealed that surface roughness of composite was inversely proportional to water pressure.

D. Sidda Reddy and A. Seshu Kumar [13] in 2014 carried out an effort to augment parameters used in Abrasive WaterJet Machining of Inconel alloy through the Taguchi methodology. The tactic was worked on the variance analysis to improve upon the efficacy of abrasive waterjet parameters for better rate of material removal and roughness of the surafce. It was also established that for surface roughness, standoff distance and transverse speed were the most important factors with 47% and 37% respectively. Whereas the abrasive flow rate was discovered to have a lesser impact on SR.

In 2016 Rajkamal Shukla and Dinesh Singh [14] undertook the experimental examination on abrasive water jet machining (AWJM) procedure using Taguchi methodology on material AA631-T6. It was aimed at examining abrasive flow rate and transverse speed to find the impact of these parameters on width of top kerf and angle of

taper. Optimization methods including artificial bee colony, particles swarm optimization, non-dominated sorting genetic algorithm, firefly algorithm, simulated annealing, biogeography based, and black hole were conducted for AWJM procedure. As a result of the confirmatory examination, both the optimization methods and the Taguchi method have been found to be valuable means in optimizing the procedure factors of the AWJM procedure.

In the year 2016, KSK Sasikumar, KP Arulshri [15] conducted an experimental enquiry on AWJ while cutting AI7075-TiC and B_4C composites. The study was based on ANOVA, which disclosed that AWJM parameters to include standoff distance, pressure of water jet and jet traverse speed had an immediate effect on kerf characteristics. The study proposed that to obtain a superior surface finish and minimum KA a higher level of water jet pressure be chosen. SEM technology was used to examine machined surfaces and ploughing marks were found during the low-level water jet pressure. Non-enmeshment of abrasive particles on the machined surface was evidenced through X-ray diffraction analysis.

In 2019 M. Boujelbene, E. Bayraktar, S. Ben Salem [16] probed the outcome of traverse speed and material thickness on width of kerf and surface integrity of titanium alloy. Surface veracity studies of micrographs, surface roughness, 3D surface topography and 2D surface roughness profiles were undertaken through alteration of thickness material and cutting speed. SEM analysis verified the existence of wear tracks caused by the AWJ cutting surfaces increasing speed which was directly proportional to cutting speed. It was found that with increased cutting speed, AWJ cut narrowed width of kerf with a bigger ratio of kerf taper on and the size of the three zones rested on the AWJ conditions and the parameters designs. It was also confirmed that, in the machined surface wall cut surface, a very minor quantity of abrasive particles was embedded.

In 2003 Y. W Seo and M Ramulu [17] carried out the examination of titanium alloy for geometry of kerf, quality of surface and microstructural integrity Microstructure features and quality of surface afer machining were examined with the support of EDX, SEM analysis and profilometry analysis. The surface roughness was evaluated at the jet exit and few micrometres close to jet entrance section of the material. It was found

during SEM test that machining process of material was blend of ploughing moment and induced ductile shear of abrasive elements.

In 2018, Gnanavel Babu and P. Saravanan [18] evaluated the optimal use of titanium alloy Ti-6AI-4V in AWJM technique factors while conducting it via evolutionary optimal methods and response surface method (RSM). Analysis of variance showed that water pressure and traverse speed are of greatest importance to surface roughness and kerf angle, in the order. Emerging optimal processing uses like SA, PSO and CSA were used to the data set to find maximum factor setting, which suggested that CSA was top optimal technique. Confirmation to this effect was certified in final test where error showed less than 3% in optimal values by CSA and values of experiment.

It was in 2019 that Sergej Hloch [19] in his research related to Abrasive Water Jetting studied the behaviour and breaking up of particles in different scenarios. The outcome was that increased fragmentation of particles at high pressure restricted that ability of abrasive jet to conduct the cutting of material. Thus, pressure was found to be utmost important element on the particle fragmentation where, kinetic power was considerably limited at higher pressure at constant abrasive flow rate.

2.4) Flow Chart for Experimentation

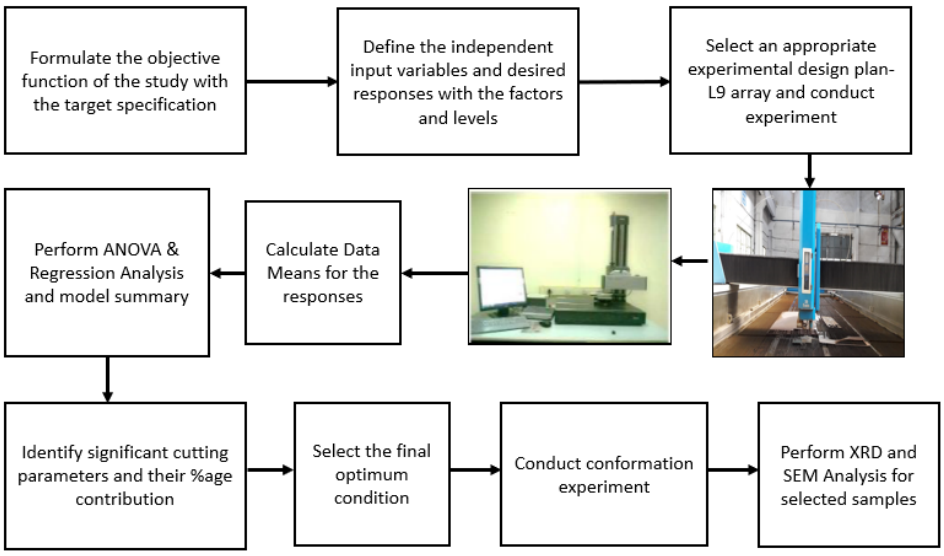

Figure 2.4 Flow chart for experimentation

2.5) Summary of Chapter

According to literature review titanium and nickel-based alloys due to high corrosion resistance, high strength and low density are more suitable for submarine and aerospace applications. However, these alloys are difficult to machine with conventional machining process due to their low thermal conductivity and high reactivity, leading to high cutting temperature and permanent tool failure. Abrasive Water Jet Machining has emerged as a fast-growing non-traditional cutting technology with several advantages which includes no heat affected zone, less cutting forces and environmental friendly. Abrasive waterjet works on principle of erosion. The course of action of abrasive waterjet machining is dealt by many process parameters such as orifice diameter, speed of traverse and water pressure. The efficiency of waterjet is measured in terms of response parameters like cutting depth, kerf angle and surface roughness. In the present era, the use of abrasive water jet technology is being commonly applied in the modern industry which includes but is not limited to construction engineering, chemical process engineering, construction engineering, automotive industry, aerospace industry and environmental technology.

Chapter 3: “Experimentation”

3.1) List of Equipment

There is different type of equipment’s used for the experimentation. This equipment can be categorized into the machining equipment, data collection equipment and analysis equipment. The details and specification of the equipment will be discussed later in the experimentation section. The list of equipment that are used for the experimentation are given below.

1. Abrasive Waterjet machine

2. Optical microscope

3. Optical Profilometer

4. Scanning electron microscope (SEM)

5. XRD machine

3.2) Work Piece Material

Inconel 600 and Titanium grade V are used in the experimentation for this research. The samples were available in the shape of circular bar with measurement of 18mm*40mm

3.3) EDS Analysis

Composition test was done for both samples with the help of scanning electron microscope to find the exact material specification. Three tests were conducted on different spots.

3.3.1) INCONEL 600

The result of the EDS analysis for Inconel 600 is given in Table 3.1. SEM image taken while composition tests and EDS spectrum is shown in Figure 3.1 & 3.2

Table 3.1

Comparison of material composition Inconel 600

Element	Nickel	Chromium	Iron	Carbon	Manganese	Cobalt	Total
% Weight	72.42	15.76	6.67	4.54	0.41	0.21	100

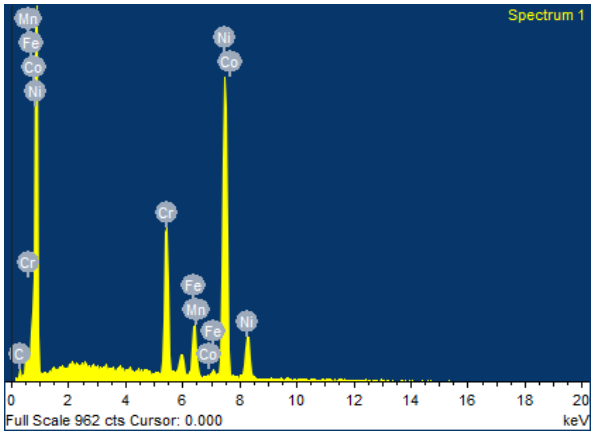

Figure 3.1 EDS spectrum of Inconel 600

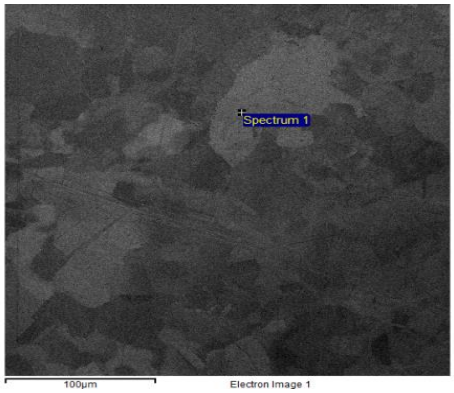

Figure 3.2 SEM image during composition test

3.3.2) Titanium Grade V

The result of the EDS analysis for Titanium grade V is given in Table 3.2. EDS spectrum and SEM image taken while composition test is shown in Figure 3.3 & 3.4

Table 3.2

Comparison of material composition Titanium grade V

Element	Titanium	Aluminium	Vanadium	Molybdenum	Palladium	Total
% Weight	90.02	7.10	2.06	0.50	0.32	100

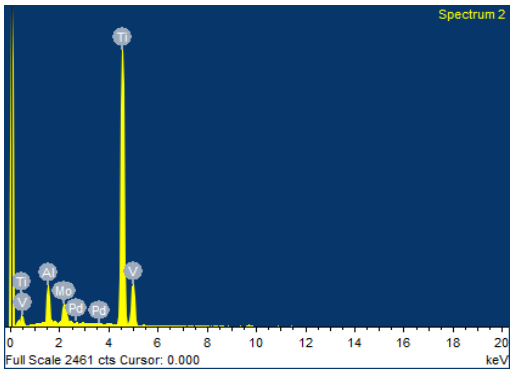

Figure 3.3 EDS spectrum of titanium grade V

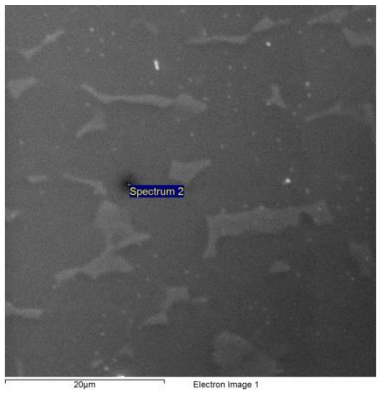

Figure 3.4 SEM image during composition test

3.4) Mechanical Properties

3.4.1) Vickers Hardness Test

Micro hardness tester is used to find the hardness of Inconel 600 and Titanium grade V. Five tests were conducted on different areas to be more accurate. Dwell time was 15 sec and 1 Kgf was used during these tests.

3.4.2) Rockwell Hardness Test

To find the Rockwell hardness of Inconel 600, 10 Kgf steel ball and for Titanium grade V diamond ball 10 Kgf is used. Five tests were conducted on different areas to be more accurate.

3.4.3) Test Results

Table 3.3

Hardness results for Inconel 600 & Titanium grade V

Material	Vickers Hardness No	Rockwell Hardness No
Inconel 600	192	81 to 82 HRB
Titanium Grade V	340 to 342	30 HRC

3.5) Abrasive Waterjet Machine

Abrasive Water Jet machine installed at Heavy Industries Taxila as shown in Figure 3.5, was used to cut samples by using different parameters for the experimentation. The specification for the Abrasive Water Jet machine is given in Table 3.4

Table 3.4

Abrasive Water Jet Machine Specification

S No	Parameter	Specification
1	Model	MTJ-W53D+40100
2	Abrasive Flow	100 gm/min to 500 gm/min
3	Nozzle dia.	0.9 mm
4	Orifice dia.	(0.25, 0.30,0.35) mm
5	Water Flow Rate	4 litres/min
6	Water Pressure	100 MPa to 500 MPa
7	Thickness	Up to 200 mm
8	Traverse Speed	1500 mm/min (max)
9	Bed Size	X = 144 in, Y = 384 in, Z = 20 in

Figure 3.5 Abrasive Water jet Machine

3.6) Abrasive Used

Abrasive materials of various typ are available in the market for use in AWJM, but garnet is mostly used and in high demand because of its easy obtainability in open market, efficacy of hardness, maximum cutting depth, flow rate and lower price [6] [4]. Abrasive Garnet 80 # was used in AWJ machine for cutting both alloys. The Composition test was for garnet using scanning electron microscope to find the exact specification of the material. Three tests were conducted on different spots. The result of the EDS analysis for garnet is given in Table 3.5. EDS spectrum and SEM image taken while composition test is shown in Figure 3.6 & 3.7. The average particle size measured from SEM analysis and laser particle size analyzer was 140 µm to 195 µm as shown in Figure 3.8

Table 3.5

Comparison of material composition for Garnet

Element	Si	Fe	C	Al	O	Mg	Mn	Ca	Total
% Weight	13.05	19.75	10.94	7.67	42.8	3.34	1.25	1.20	100

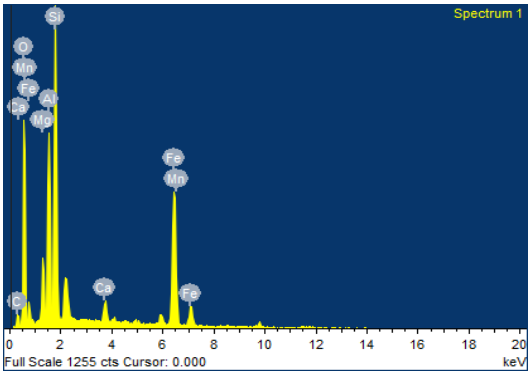

Figure 3.6 EDS spectrum of garnet

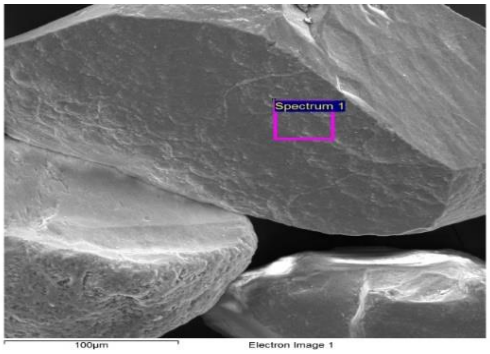

Figure 3.7 SEM image during composition test

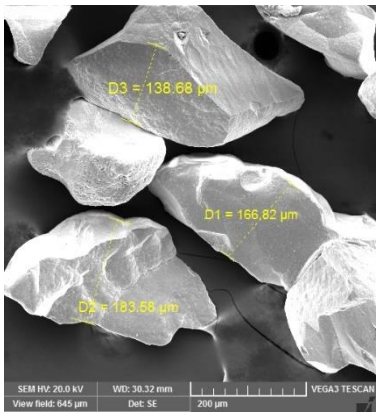

Figure 3.8 SEM image for particle size

3.7) Selection of Process Parameters

Surface roughness, kerf taper, material removal rate, and depth of cut have all been considered responses, but researchers have discovered that traverse speed, water pressure, nozzle diameter, abrasive flow rate, and standoff distance are the most important variables in the AWJM process.

The following criteria are used for the selection of different level of parameters.

3.7.1) Traverse Speed (mm/min)

Cutting at slow traverse speed is recommended by researchers because increased traverse speed indicates a considerable growth in kerf angle and a decrease in smooth cutting by one-quarter of the whole cutting section of the material [10]. Keeping in view the large size of the AWJ machine in comparison to the smaller size of the sample, a low-level traverse speed was selected. The sample could have been affected with high traverse speed settings, so the selected Traverse speed was 2mm/min, 4mm/min and 6mm/min.

3.7.2) Water Pressure (MPa)

The increase in pressure of water jet will result in decrease in kerf angle. Pressure of the water jet is the utmost determining feature linked to the morphology of removal of material and surface finish. To achieve a good surface finish for superalloys machining should be done at moderate traverse speed and high-water pressure [20]. Water pressure was set on a little higher side (500MPa) by default, as the minimum interval between the water pressures was 100 MPa. Whereas available ranges were between100 – 600 MPa

but the nozzle was choking below 300 MPa. Selected water pressure levels were 300MPa, 400Mpa and 500 MPa.

3.7.3) Abrasive Flow Rate (gm/min)

The quantity of impacting abrasive particles along with the overall kinetic energy accessible is determined by abrasive flow rate determines and have most significant influence on kerf angle and surface roughness. The available range for abrasive flow rate was 100 to 500 gm/min. Selected levels were 200 gm/min, 250gm/min and 300 gm/min. At lower abrasive flow rate cutting will not be initiated and increased abrasive flow rate will increase the cost of the process [11]

3.7.4) Stand-off Distance (mm)

The stand-off distance is usually retained in a span of 1 to 5 mm. Enhancing stand-off distance will enlarge kerf angle and surface roughness as a consequence of the divergence of the jet, whereas minor values will generate phenomena of back pressure [3]. Selected values were 2mm, 3mm and 4mm. The parameters selected with their levels for the AWJ machining of Inconel 600 and Titanium grade V is given in the below Table 3.6.

Table 3.6

Processes parameter with levels

Parameter	Units	Level 1	Level 2	Level 3
Traverse Speed (TS)	mm/min	2	4	6
Water Pressure (WP)	MPa	300	400	500
Abrasive Flow Rate (AFR)	gm/min	200	250	300
Stand-off Distance (SOD)	Mm	2	3	4

3.8) Design of Experiments

This method offers an efficient as well as a simple and methodical approach for a best possible design to excess the performance, cost and quality. This design of experiments was utilized to cut down the number of experiments to optimize cost and time [11]. Based on levels of process parameters and a Taguchi L9 orthogonal array is used to define 9 trials by using MINITAB 19 software. The experimental layout is given below in Table 3.7

Taguchi Array L9(3^4)

Factors: 4

Runs: 9

Table 3.7

Experimental plan using an L9 orthogonal array

S No	Traverse Speed (TS) mm/min	Abrasive Flow Rate (AFR) gm/min	Water Pressure (WP) MPa	Stand Off Distance (SOD) mm
1	2	200	300	2
2	2	250	400	3
3	2	300	500	4
4	4	250	300	4
5	4	300	400	2
6	4	200	500	3
7	6	300	300	3
8	6	250	400	4
9	6	200	500	2

3.9) Methodology

The experiments were done on Inconel 600 and Titanium grade V using Abrasive Water Jet Machine with impact angle of 90 degree and thickness of 4 mm. As an abrasive, garnet with 80 mesh was employed. Nozzle diameter was 0.9 mm. Orifice diameter (diamond) was taken as 0.30 mm because to obtain optimum performance and good depth of cut, a ratio of 3 to 4.5 between nozzle to orifice diameter is recommended [9]. Total 36 samples were cut for each alloy by cutting four samples against each combination from experimental plan (L9 Array) obtained from DOE. For kerf analysis a

horizontal cut of 9 mm was made on 18 samples for each alloy as shown in Figure 3.9 and Table 3.8 shows experimental conditions for these tests.

Table 3.8

Experimental Conditions for AWJM

Workpiece	Inconel 600 & Titanium Grade V
Diameter of Nozzle	0.9 mm
Diameter of Orifice (Diamond)	0.3 mm
Cutting Thickness	4 mm

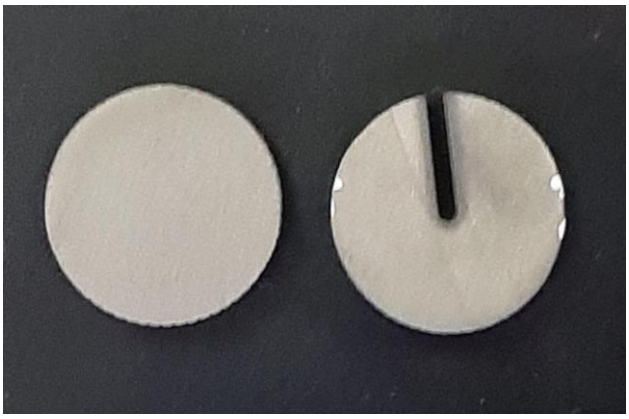

Figure 3.9 Samples after AWJ Machining

3.10) Measurement of Response Parameters

Following response parameters were selected.

3.10.1) Kerf Angle (degrees)

The geometry of Kerf is an attribute of key concern in AWJ cutting as it generally opens a slot which is tapered. The top width (Wt) is broader than the width of the bottom (Wb) as shown in Figure 3.10. The perpendicularity or straightness of the cut gets worse by the larger kerf angles which results in inaccurate dimensional quality [21]

Wt = Top width of kerf

Wb = Bottom width of kerf

t = Thickness of sample

t = 4 mm

kerf angle = $\Theta = \tan^{-1} (Wt-Wb)/2t$____equation (1)

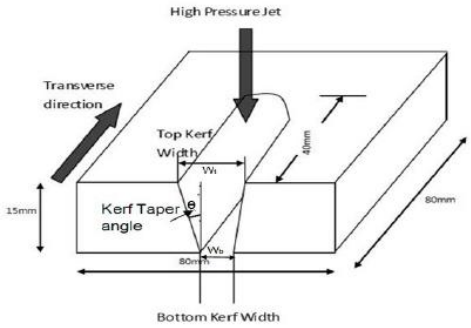

Figure 3.10 AWJM Cut

The measurement of width of top kerf (Wt) and width of bottom kerf (Wb) was done with the help of Optical microscope using lens 5X and kerf angle was computed with the help of equation 1. Two values for kerf angle were recorded per specimen and their mean value was used for kerf analysis. Images recorded from optical microscope for sample of Inconel 600 are shown in Figure 3.11 (a) & (b).

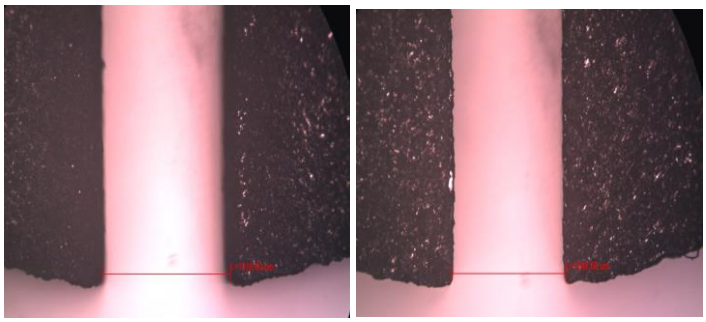

(a) Top kerf width sample I 9/2 Wt = 1516 µm

(b) Bottom kerf width sample I 9/2 Wb = 1348 µm

Figure 3.11 Images from optical microscope

3.10.2) Surface Roughness (µm)

The inherent irregularities of machined material influenced by abrasive particles contact is regarded as the surface roughness. Surface roughness performs a vital part in obtaining dimensional accuracy therefore; choice of process parameters is of utmost importance for acquiring superior surface finish. Surface roughness was measured using an Optical profilometer PS Nanovea 50. Two readings were recorded against each set of L9 array and mean value was considered for analysis. Surface roughness values were measured in micrometers. Surface roughness profile of a sample is shown in Figure 3.12 with surface roughness value of 2.66µm and scan length of 10mm.

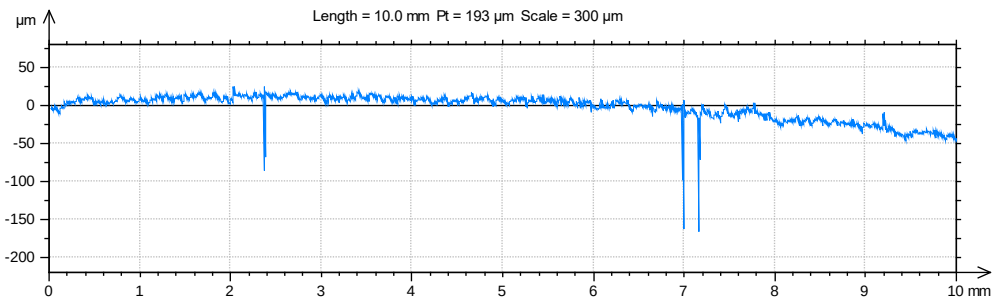

Figure 3.12 Surface roughness profile of Sample I-1/4

3.11) Taguchi Methodology

To reduce time and improve upon efficiency during study and progression timeframe use of Taguchi technique in recent years has increased manifolds. It is a technique which gives an easy, effective, logical, and orderly style for attaining best results in terms of efficacy and expenses [22]

3.11.1) Variance Analysis (ANOVA)

ANOVA was achieved with the aid of MINITAB 19 software to investigate the outcome of parameters of machining on kerf angle and surface roughness with the help of %age contribution. For a 95% confidence level ($\alpha = 0.05$), a detailed analysis was carried out. Based on these results the significance of machining parameters on kerf angle and surface roughness was calculated.

3.11.2) Regression Analysis

This analysis is used to evaluate regression coefficients that minimize the error and predictions from the developed regression models were compared with measured kerf angle along with surface roughness. The insignificant parameters were pooled out from regression analysis. Regression equations were obtained for surface roughness as well as kerf angle after analyzing the impact of all individual parameters. This mathematical model provides a good relationship between parameters of machining and response parameters. The capability of the model was tested with the help of coefficient of determination R^2.

3.12) SEM Analysis

3.12.1) Sample Preparation

The following steps were adopted for the sample preparation before conducting SEM analysis.

3.12.2) Sample Cutting

To study the microstructural changes along the border of the sample and to get a small flat surface to facilitate the mounting process a small section of sample was cut using hand saw as shown in Figure 3.13

(a) Sample after AWJ cutting (b) Sample after hand saw cut

Figure 3.13 Machined sample before mounting

3.12.3) Sample Mounting

For analyzing the microstructure, first we need to make a mold in which sample was placed. For making the mold, mounting mechanism is the most appropriate method. Sample was place on the vertical placement bar of "Hydro- press Mounting Machine" which is also called Automatic Mounting Machine. Shower the specific amount of Conductive mount Bakelite powder over the sample and covered the mounting press with a plunger. Set the temperature T (Su) of 180^{o}C and pressure 270 bar, wait for 20 minutes to achieve the mounted sample. After completion of cycle, machine beep would be heard, which is basically the indication to collect your sample specimen as shown in Figure 3.14. This process was repeated for all selected samples.

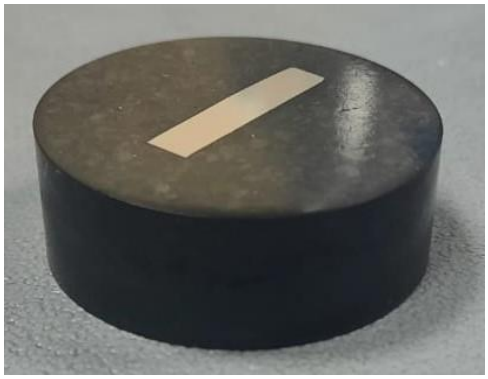

Figure 3.14 Mounted Sample

3.12.4) Sample Grinding

Mounted samples were then grinded by using different abrasive grinding papers, i.e. Silicon Carbide (waterproof) grinding papers with the help of automatic grinding and polishing machine. The various parameters for machine setting are given in Table 3.9. First, the mounted samples were grinded by using 320 and 800 silicon carbide grinding papers to trim mold surface. Then shifted to 1200, 2000 and 2400 at the end when the surface was nearly finished (smooth), 4000 abrasive grinding paper was used. When shifting the mounted sample from one silicon carbide grinding paper to another it was washed with water and ethanol.

Table 3.9

Machine setting for grinding mounted samples

Grinding Force	Time	RPM Head	RPM Bed
3 DaN	3 min onwards	250	150

3.12.5) Sample Polishing

Polishing of the mounted samples was done using automatic grinding and polishing machine. Extra fine and smooth surface was the main objective. Polishing pads from 3 µm to 0.05 µm were used along with their respective colloidal suspensions. When shifting the mounted sample from one polishing paper to another it was washed with water and ethanol and surface was observed using optical microscope at each stage. Various machine parameter settings along with the time taken for polishing against each polishing pad in given in Table 3.10.

Table 3.10

Machine setting for polishing of mounted samples

Polishing Pads	Grinding Force	Time	RPM Head	RPM Bed
3 µm	1.5 DaN	10 min	150	100
1 µm	1.5 DaN	10 min	150	100
0.5 µm	1.5 DaN	20 min	150	100
0.05 µm	1.5 DaN	300 min	150	100

Scanning electron microscopy was done for selected samples of both alloys to measure the grain distortion after Abrasive water jet machining using Image J software.

3.13) XRD Analysis

Diffraction of X-rays from crystal structure is a strong technique to determine lattice planes, stress, strain, and phases. X-rays are high energy waves, which when collide to a material, are scattered according to the atomic locations in the crystal. This is due to periodic arrangement of atoms. Scattered rays which are out of phase show destructive interference. The XRD analysis was done using Xpert PRO PANalytical machine to check the phase changes and entrapment of abrasive particles in machined samples. The wavelength used was 1.54 Angstrom and source was Copper tube.

3.14) Summary of Chapter

Inconel 600 and Titanium grade V are selected for this research and composition test was done for both alloys to find the exact material specification. Micro hardness tester is used to find the hardness of Inconel 600 and Titanium grade V. Based on levels of process parameters a Taguchi L9 orthogonal array is used to define 9 trials by using MINITAB 19 software. Abrasive Water Jet machine installed at Heavy Industries Taxila, is used to cut samples by using different parameters for the experimentation. Abrasive Garnet 80 # was used in AWJ machine for cutting both alloys. The measurement of width of top kerf (Wt) and width of bottom kerf (Wb) was done with the help of Optical microscope while surface roughness was measured using an Optical profilometer. Samples were mounted, grinded and polished to conduct SEM analysis.

Chapter 4:

"Abrasive Water Jet Cutting of Inconel 600"

4.1) Introduction

Abrasive Water Jet machine installed at Heavy Industries Taxila, is used to cut samples by using different parameters for the experimentation with impact angle of 90 degree and sample thickness of 4 mm. Taguchi L9 orthogonal array is used to define 9 trials by using MINITAB 19 software. Total 36 samples were cut, four samples against each combination from experimental plan as shown in Table 3.7. For kerf analysis a horizontal cut of 9 mm was made on 18 samples and the measurement of width of top kerf (Wt) then width of bottom kerf (Wb) was done using Optical microscope.

4.2) Kerf Angle Results

Results for kerf angle for Inconel 600 were calculated with the help of equation 1 are presented in Table 4.1 below.

Table 4.1
Results of kerf angle

S No	Sample No	TS mm/min	WP MPa	AFR gm/min	SOD mm	KF degrees
1)	In (1)/1	2	300	200	2	1.0786
2)	In (2)/1	2	400	250	3	1.1345
3)	In (3)/1	2	500	300	4	1.552
4)	In (4)/1	4	300	250	4	1.4398
5)	In (5)/1	4	400	300	2	1.3635
6)	In (6)/1	4	500	200	3	1.575
7)	In (7)/1	6	300	300	3	1.3789
8)	In (8)/1	6	400	200	4	1.6496
9)	In (9)/1	6	500	250	2	1.6905

4.2.1) Response Table for Data Means

Data mean values and ranking of process parameters is given in Table 4.2 which shows that traverse speed is most important factor for kerf angle.

Table 4.2
Response table for mean kerf angle

Level	TS	WP	AFR	SOD
1	1.254	1.299	1.434	1.379
2	1.459	1.383	1.423	1.363
3	1.574	1.606	1.431	1.546
Delta	0.320	0.307	0.012	0.184
Rank	1	2	4	3

4.2.2) Variance Analysis

Variance analysis is used to discover the major process parameters as shown in Table 4.3. Traverse speed and water pressure comes out to be the most substantial process parameters affecting kerf angle. As contribution of abrasive flow rate (AFR) was less than 1 % and it is on rank 4 as shown in Table 4.2, so it was pooled out.

Table 4.3
Variance analysis for kerf angle

Source	DF	Adj SS	Adj MS	Contribution	F-Value	P-Value	Significance
Regression	3	0.33722	0.112405		16.50	0.005	
TS	1	0.15341	0.153408	42.41 %	22.52	0.005	Significant
WP	1	0.14159	0.141588	40.78 %	20.79	0.006	Significant
SOD	1	0.04222	0.042218	16.73 %	6.20	0.055	Not significant
Error	5	0.03406	0.006812				
Total	8	0.37127					

4.2.3) Regression Equation

Regression equations is obtained for kerf angle after analyzing the impact of all individual parameters, providing a good relationship between machining parameters and output parameters.

Kerf Angle = 0.243 + 0.0799 TS + 0.001536 WP + 0.0839 SOD

4.2.4) Model Summary

The values of R^2 and R^2 adjusted are between 85 to 90 % as shown in Table 4.4. This shows that regression model provides a good relationship between process and response parameters.

Table 4.4
Model summary for kerf angel

S	R-sq	R-sq (adj)	R-sq (pred)
0.0825321	90.83%	85.32%	72.12%

4.2.5) Data Means Plot

The mean effect of data means plot is shown in Figure 4.1 showing effect of process parameters on response parameters.

Figure 4.1 Data means plot for kerf angle

4.3) Kerf Angle Analysis

The plot for data means in Figure 4.1 displays the deviation of kerf angle in connection with other selected process parameters

4.3.1) Traverse Speed (TS)

The kerf angle increases with growing traverse speed from 2mm/min to 6mm/min because there is an association between the increase in traverse speed and reduction in the interaction of jet on a specific area of material which directs to material erosion by smaller number of abrasive particles. Therefore, lower traverse speed leads to smaller kerf angles and is the most significant factor while machining nickel-based alloys [21] [23]. For Inconel 600, traverse speed is the leading factor that affects the kerf angle values which is almost 42% of the total variability as shown in Table 4.3. Traverse speed is found to be the significant parameter because the P-values was less than 0.05 which means the confidence level is 95% or above.

4.3.2) Water Pressure (WP)

Water pressure was to be the next important factor affecting kerf angle values with almost 40% of the total variability having P-value which is less than 0.05 as shown in Table 4.3. It can be comprehended that the kerf angle increases as water pressure increments from initial 300MPa to 500MPa. In general, the kerf angle decreases as the water pressure goes up since the cutting ability of the jet rises at higher pressure. Some investigations show that the relationship between water pressure and kerf angle becomes linear with a negative effect, contrary to conventional findings. It is also claimed that there's a critical pressure that's comparable to the material's lowest cutting pressure, and that this critical pressure climbs as the material's strength increases. Secondly, increasing water pressure reduces hydraulic efficiency and causes particle disintegration as they depart the nozzle. Because smaller particles lose their kinetic energy sooner, increased fragmentation diminishes the cutting efficacy of abrasive particles. As a result, with higher water pressures, bigger kerf angles can be obtained. [24] [22] [19]

4.3.3) Abrasive Flow Rate (AFR)

The change in kerf angle as the flow rate of abrasive is enhanced from 200gm/min to 300gm/min is very slight and influence is not as noteworthy as compared to other process factors and hence pooled out while regression analysis.

4.3.4) Standoff Distance (SOD)

There is a slight change in kerf angle since standoff distance grows from 2mm to 3mm but for 3mm to 4mm, there is a rapid increase in kerf angle. Higher standoff distance expands the jet diameter as cutting is initiated, which lowers the kinetic energy of jet and effective cutting area resulting in larger kerf angles. Standoff distance is found to be not significant for kerf taper angle with 16.7 % contribution and the P-value was not less than 0.05.

4.4) Optimal Process Parameters

Thus, the optimal setting of Inconel 600 for obtaining minimum kerf angle is given in table 4.5

Table 4.5
Optimal process parameters for kerf angle

Process Parameter	TS (mm/min)	WP (MPa)	AFR (gm/min)	SOD (mm)
Optimal Setting	2	300	250	3

4.5) Surface Roughness Results

Surface roughness was measured using an Optical profilometer and two readings were recorded against each set of L9 array and mean value of Ra (µm) was considered for analysis. Table 4.6 depicts the results for surface roughness**.**

Table 4.6
Results for surface roughness

S/No	Sample No	TS mm/min	WP MPa	AFR gm/min	SOD mm	Mean (Ra) µm
1)	In (1)/3	2	300	200	2	2.77
2)	In (2)/3	2	400	250	3	3.13
3)	In (3)/3	2	500	300	4	3.85
4)	In (4)/3	4	300	250	4	2.95
5)	In (5)/3	4	400	300	2	3.165
6)	In (6)/3	4	500	200	3	3.62
7)	In (7)/3	6	300	300	3	2.82
8)	In (8)/3	6	400	200	4	3.48
9)	In (9)/3	6	500	250	2	3.74

4.5.1) Response Table for Data Means

Ranking of process parameters and data mean values is given in Table 4.7, which shows that water pressure being on rank 1 is most important factor for surface roughness.

Table 4.7
Response table for mean surface roughness

Level	TS	WP	AFR	SOD
1	3.250	**2.847**	3.290	3.223
2	**3.243**	3.257	**3.273**	**3.190**
3	3.347	3.737	3.277	3.427
Delta	0.103	0.890	0.017	0.237
Rank	3	1	4	2

4.5.2) Variance Analysis

To detect the major process parameters and their %age contribution variance analysis is done as shown in Table 4.8. Water pressure comes out to be the highly significant process parameter that affects surface roughness. Standoff distance is also sub significant with p value less than 0.05.

Table 4.8
Variance analysis for surface roughness

Source	DF	Adj SS	Adj MS	Contribution	F-Value	P-Value	Significance
TS	1	0.01402	0.01402	1.53 %	1.54	0.269	Not Significant
WP	1	1.18815	1.18815	90.91 %	130.81	0.000	Significant
SOD	1	0.06202	0.06202	7.5 %	6.83	0.048	Significant
Error	5	0.04542	0.00908				
Total	8	1.30960					

4.5.3) Regression Equation

Regression equation shown below is obtained for surface roughness.

Surface roughness = 1.098 + 0.0242 TS + 0.004450 WP + 0.1017 SOD

4.5.4) Model Summary

The values of R^2 and R^2 adjusted are above 90 % as shown in Table 4.9. This shows that regression model provides an excellent relationship between process and response parameters.

Table 4.9
Model summary for surface roughness

S	R-sq	R-sq(adj)	R-sq(pred)
0.0953065	96.53%	94.45%	86.57%

4.5.5) Data Means Plot

The mean effect of data means plot is shown in Figure 4.2 showing effect of process parameters on response parameters.

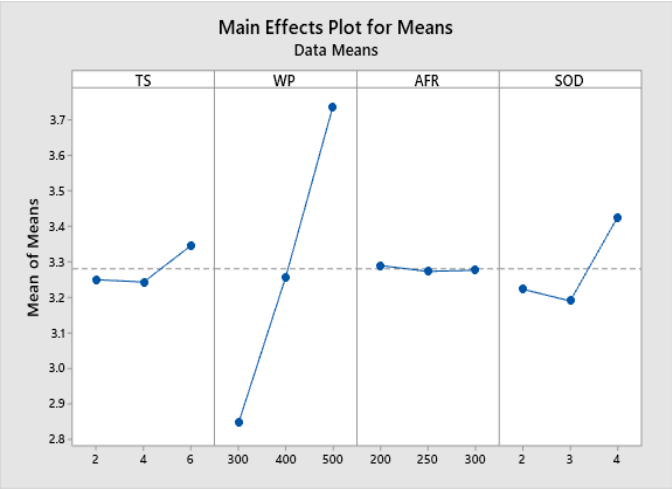

Figure 4.2 Data means plot for surface roughness

4.6) Surface Roughness Analysis

The data means plot in Figure no 4.2 demonstrates the deviation of surface roughness relating to other selected process parameters explained as under,

4.6.1) Traverse Speed (TS)

Surface roughness increases slightly when traverse speed goes from 2mm/min to 4mm/min, and then increases further as traverse speed increases from 4mm/min to 6mm/min. Higher traversal speeds result in a reduced amount of abrasive particles participating in action of cutting, which increases surface roughness. To obtain the lowest surface roughness cutting at a lower traverse speed should be opted

4.6.2) Water Pressure (WP)

Surface roughness increases with the increase in water pressure from 300MPa to 500MPa. Generally, the surface roughness decreases with increases in water pressure but as the water pressure reaches above its critical limit, in many cases it shows decreased cutting performance due to the increased fragmentation of abrasive particles [19][22]. Water pressure is a highly influential factor related to surface finish [20] with maximum contribution of 90 % and P-value less than 0.05.

4.6.3) Abrasive Flow Rate (AFR)

The influence of abrasive flow rate is not as significant regarding other process parameters as there is a slight variation in surface roughness with the increase in abrasive flow rate from 200gm/min to 300gm/min and is pooled out from regression analysis.

4.6.4) Stand-off Distance (SOD)

There is a trivial change in surface roughness as standoff distance transforms from 2mm to 3mm and afterwards surface roughness rises as the standoff distance increases. Higher standoff distance decreases energy density of jet resulting in lower penetration of jet which increases surface roughness. Secondly, a larger standoff distance may cause external drag from surrounding which will increase jet diameter and reduces the jet energy. Standoff distance is a significant factor for surface roughness with a P value less than 0.05

4.7) Optimal Process Parameters

Thus, the optimal setting of Inconel 600 for surface roughness is given in Table 4.10

Table 4.10
Optimal process parameters for surface roughness

Process Parameter	TS (mm/min)	WP (MPa)	AFR (gm/min)	SOD (mm)
Optimal Setting	4	300	250	3

4.8) Analysis for Abrasive Entrapment

4.8.1) XRD Analysis

To verify the entrapment of garnet, XRD of Inconel 600 was done. The wavelength used was 1.54 Angstrom and source was Cu K. XRD pattern of Inconel 600, machined sample is shown in Figure 4.3. All the peaks of samples belong to Inconel 600 and no additional peaks were seen. This may be due to the reason that entrapment of abrasive garnet was very less in the form of small peaks which may disappear during smoothing process or removing noise level from graph. Secondly if the contribution of an element is less than 1% then it is not detected in XRD analysis.

4.8.2) SEM Analysis

To further investigate the garnet embedment on machined surface, machined sample at highest surface roughness (3.85 μm) was observed using SEM analysis as shown in Fig 4.4 and further confirmation for embedded particles has been made through the EDS analysis of the AWJ machined sample. The chemical composition of AWJ machined sample shown in Table 4.11 and as received sample shown in Table 3.1 is compared and it is observed that Silicon, Magnesium, and Calcium elements were found in the chemical composition of AWJ machined sample which were same as per chemical composition of abrasive garnet as shown in Table 3.5. This confirms the abrasive particles entrapment in the machined samples. It is difficult to remove the embedment of abrasive particles in the workpiece, resulting in low fatigue life and can be reduced by post-processing [25] using soluble abrasives [26] or by reducing impact angle for AWJ milling [27].

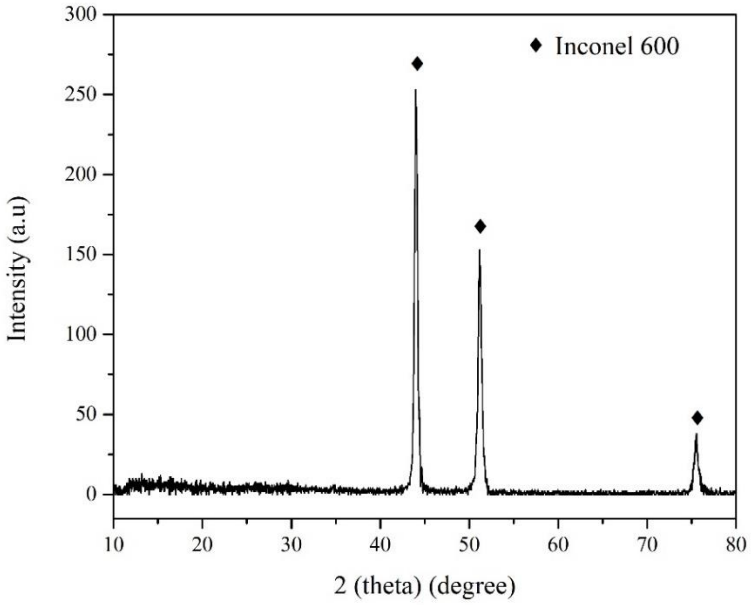

Figure 4.3 XRD pattern for Inconel 600

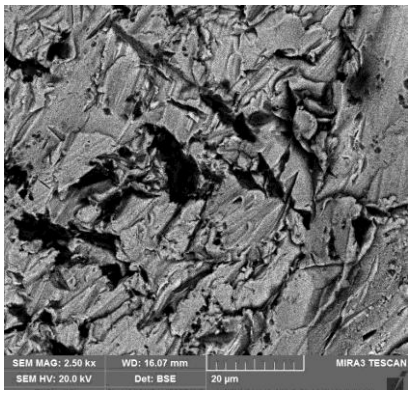

Figure No 4.4 SEM image of machined sample

Table 4.11
Chemical composition of AWJ machined sample

Element	Ni	Cr	Fe	C	Si	Mg	Al	Ca
Wt %	60.50	15.71	6.72	14.57	0.53	0.36	1.50	0.10

4.9) Grain Distortion Measurement

Selected machined samples were mounted, grinded and polished before conducting SEM analysis for measuring grain distortion. Grain distortion of machined samples is measured at three different points along the boundary line using ImageJ software shown in Table 4.12 Fig 4.5 shows the surfaces from the SEM backscatter detector at minimum and maximum water jet pressure. The image shows a very trivial influence down to a few micrometres under the machined surface. An increase in grain distortion is observed from 18.72 µm to 40.74 µm as surface roughness is increased from 2.77µm at to 3.85µm respectively. As water pressure came to be the utmost prominent factor for surface roughness for Inconel 600, hence there is an increase in average size of grain distortion and surface roughness with the increases in the water pressure. The reason for this deformation could be due to the bombardment of abrasive particles at high energy, which increases as the water pressure increases. A lower value of grain distortion is obtained at water pressure at 300 MPa and traverse speed of 2 mm/min.

Table 4.12
Grain distortion of AWJ machined samples

S/No	Sample No	TS mm/min	WP MPa	AFR gm/min	SOD mm	Ra µm	Grain Distortion µm
1)	In (1)	2	300	200	2	2.88	18.721
2)	In (8)	6	400	200	4	3.48	25.813
3)	In (3)	2	500	300	4	3.85	40.74

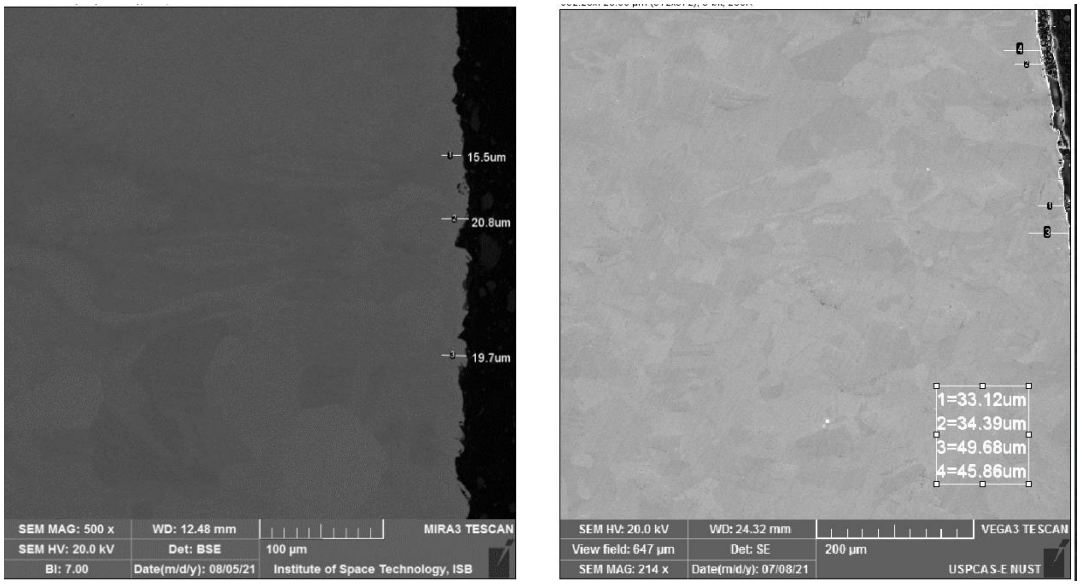

(a) Grain distortion at 300MPa (b) Grain distortion at 500MPa

Figure 4.5 Grain distortion of machined surface

4.10) Summary of Chapter

Results for kerf angle and surface roughness for Inconel 600 were calculated. To discover major process parameters that affect the surface roughness and kerf angle, the Taguchi technique, together with variance analysis (ANOVA) were used which shows traverse speed and water pressure as major factors for kerf angle and water pressure is most influential for surface roughness. Regression equations is obtained for kerf angle after analysing the impact of all individual parameters, providing a good relationship between machining parameters and output parameters. The plot for data displays the deviation of kerf angle and surface roughness in connection with other selected process parameters. The optimal setting for process parameters were found for kerf angle and surface roughness. No additional peaks were found in the XRD analysis and entrapment of abrasive particles in machined samples is confirmed by SEM and EDS analysis. Scanning electron microscopy for grain distortion shows that lower values of water pressure will result in reduced grain distortion.

Chapter 5:

"Abrasive Water Jet Cutting of Titanium Grade V"

5.1) Introduction

Taking advantage of Abrasive Water Jet Machine installed at Heavy Industries Taxila, experiments were carried out to cut samples by adopting various considerations with impact angle of 90 degree while sample thickness was 4 mm. MINITAB 19 software helped defining the L9 orthogonal array. A total of 36 samples were cut, four sample were taken for each combination from experimental plan as shown in Table 3.7. A horizontal cut of 9 mm was made on 18 samples for kerf analysis. Whereas, the measurement of width of top (Wt) and bottom kerf (Wb) was carried out with the help of Optical microscope and kerf angle (degrees) was evaluated using equation 1.

5.2) Kerf Angle Results

Kerf angle for Titanium grade V is calculated from width of top (Wt) and bottom kerf (Wb) using equation 1 and results are presented in Table 5.1 below.

Table 5.1
Results for kerf angle

S No	Sample	TS	WP	AFR	SOD	Kerf Angle (Ɵ)
	NO	mm/min	MPa	gm/min	mm	Degrees
1)	T (1)/1	2	300	200	2	0.57285
2)	T (2)/1	2	400	250	3	0.4468
3)	T (3)/1	2	500	300	4	0.6474
4)	T (4)/1	4	300	250	4	0.7505
5)	T (5)/1	4	400	300	2	0.5843
6)	T (6)/1	4	500	200	3	0.6073
7)	T (7)/1	6	300	300	3	0.859
8)	T (8)/1	6	400	200	4	1.157
9)	T (9)/1	6	500	250	2	1.14

5.2.1) Response Table for Data Means

Data mean values and ranking of process parameters is given in Table 5.2. Traverse speed being on rank 1 turns out to be most important factor.

Table 5.2
Response table for mean kerf angle

Level	TS	WP	AFR	SOD
1	0.5620	0.7402	0.7798	0.7664
2	0.6474	0.7361	0.7858	0.6564
3	1.0641	0.7971	0.7078	0.8506
Delta	0.5021	0.0610	0.0780	0.1942
Rank	1	4	3	2

5.2.2) Variance Analysis

Variance analysis is done to detect the major process parameters as shown in Table 5.3. Traverse speed comes out to be the most significant. Water pressure was not considered as it is on rank 4^{th} with contribution of 1.38 %.

Table 5.3
Variance analysis for kerf angle

Source	DF	Adj SS	Adj MS	Contribution	F-Value	P-Value	Significance
Regression	3	0.396566	0.132189		5.92	0.042	
TS	1	0.378157	0.378157	85.2 %	16.93	0.009	Significant
AFR	1	0.007783	0.007783	2.22 %	0.35	0.581	Not Significant
SOD	1	0.010626	0.010626	11.2 %	0.48	0.521	Not Significant
Error	5	0.111686	0.022337				
Total	8	0.508251					

5.2.3) Regression Equation

Regression equation is obtained to develop a relationship between process parameters and response parameters.

$$\text{Kerf Angle} = KF = 0.310 + 0.1255\ TS - 0.00072\ AFR + 0.0421\ SOD$$

5.2.4) Model Summary

The values of R^2 and R^2 adjusted are between 78 to 65 % as shown in Table 5.4. This shows that regression model provides a reasonable relationship between process and response parameters.

Table 5.4
Model summary for kerf angle

S	R-sq	R-sq(adj)	R-sq(pred)
0.149456	78.03%	64.84%	20.53%

5.2.5) Data Means Plot

Data means plot for kerf angle is shown in Figure 5.1 represents the deviation of response parameters with respect to process parameters.

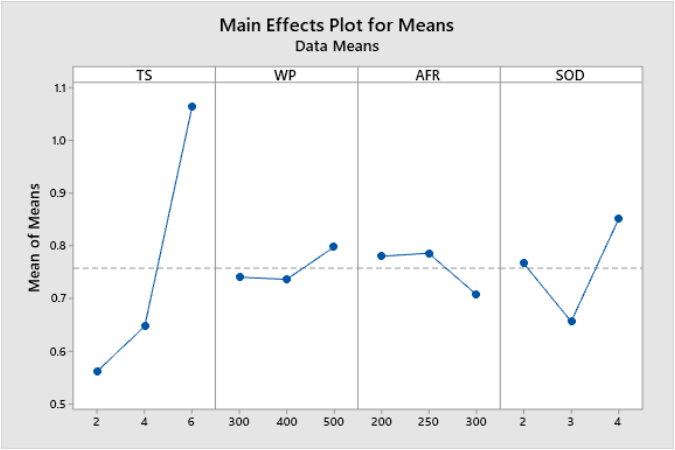

Figure 5.1 Data means plot for kerf angle

5.3) Kerf Angle Analysis

The data means plot in Figure 5.1 shows the deviation of kerf angle related to other selected process parameters.

5.3.1) Traverse Speed (TS)

With increasing traverse speed from 2mm/min to 6mm/min the kerf angle also increases. At increased traverse speed the lower part of the kerf becomes wide due to decreased jet energy as it traverses the part which in turn increases the kerf angle. Thus, for titanium grade V, speed of traverse is the highly foremost factor that affects the kerf angle values which is almost 85.2% of the total variability as shown in Table 5.3. Traverse speed is found to be the significant parameter because the P-values were less than 0.05 which means the confidence level is 95% or above.

5.3.2) Water Pressure (WP)

There is a negligible change in kerf angle with increase in water pressure from 300MPa to 400MPa and then kerf angle increases slightly as water pressure increases from 400MPa to 500MPa. Water pressure has a very low contribution towards kerf angle and is ranked 4 so it was pooled out from regression analysis.

5.3.3) Abrasive Flow Rate (AFR)

The change in kerf angle is increased with the increase in abrasive flow rate from 200gm/ min to 250gm/ min is very slight and then kerf angle decreases with the increase in abrasive flow is from 250gm/ min to 300gm/ min. Abrasive flow rate defines the amount of impacting abrasive particles and total available kinetic energy. At greater abrasive flow rate there will be more abrasive particles on unit area of cutting surface to remove more material throughout the width which will produce lower kerf values. Abrasive flow rate is non-significant for kerf taper angle as P-value is larger than 0.05 with a contribution of 2.22 % as shown in Table 5.3

5.3.4) Stand-off Distance (SOD)

There is a slight change in kerf angle as stand-off distance increases from 2mm to 3mm, but as standoff distance is increased from 2mm to 4mm there is a rapid increase in kerf angle. Diameter of the jet increases as cutting is commenced at higher values of standoff distance, which reduces kinetic energy of jet and effective cutting area resulting in larger kerf angles. Stand-off distance is found to be non-significant with contribution of 11.2 % and P-value greater than 0.05.

5.4) Optimal Process Parameters

Thus, the optimal setting of Titanium grade V for obtaining minimum kerf angle is given in Table 5.5

Table 5.5
Optimal process parameters for kerf angle

Process Parameter	TS (mm/min)	WP (MPa)	AFR (gm/min)	SOD (mm)
Optimal Setting	2	400	300	3

5.5) Surface Roughness Results

Results for surface roughness (Ra) obtained from optical profilometer for Titanium grade V are shown in Table 5.6

Table 5.6
Results for surface roughness

S/No	Sample No	TS mm/min	WP MPa	AFR gm/min	SOD mm	Mean (Ra) µm
1)	T (1)/3	2	300	200	2	2.3300
2)	T (2)/3	2	400	250	3	2.1250
3)	T (3)/3	2	500	300	4	3.0200
4)	T (4)/3	4	300	250	4	4.0550
5)	T (5)/3	4	400	300	2	2.4600
6)	T (6)/3	4	500	200	3	2.7700
7)	T (7)/3	6	300	300	3	3.5500
8)	T (8)/3	6	400	200	4	4.8400
9)	T (9)/3	6	500	250	2	3.8150

5.5.1) Response Table for Data Means

Data mean values and ranking of process parameters is given in Table 5.7 which shows that traverse speed being on rank 1 is most important factor regarding surface roughness.

Table 5.7
Response table for mean surface roughness

Level	TS	WP	AFR	SOD
1	2.493	3.313	3.313	2.870
2	3.097	3.143	3.337	2.817
3	4.070	3.203	3.010	3.973
Delta	1.577	0.170	0.327	1.157
Rank	1	4	3	2

5.5.2) Variance Analysis

To find the significant process parameters variance analysis is done as shown in Table 5.8. Traverse speed and water pressure comes out to be the major significant process parameters. Standoff distance comes out to be sub significant with P value less than 0.05

As contribution of water pressure (WP) was less than 1 % and it is on rank 4 as shown in Table 5.8, so it was pooled out.

Table 5.8
Variance analysis for surface roughness

Source	DF	Adj SS	Adj MS	Contribution	F-Value	P-Value	Significance
TS	1	3.7288	3.7288	57.54 %	20.57	0.006	Significant
AFR	1	0.1380	0.1380	3.01 %	0.76	0.423	Not Significant
SOD	1	1.8260	1.8260	38.76 %	10.07	0.025	Significant
Error	5	0.9063	0.1813				
Total	8	6.5992					

5.5.3) Regression Equation

Regression equations is obtained for surface roughness after analysing the impact of all individual parameters, providing a good relationship between machining parameters and output parameters

Surface Roughness = SR = 0.75 + 0.3942 TS – 0.00303 AFR +0.552 SOD

5.5.4) Model Summary

The values of R^2 and R^2 adjusted are between 78 to 86 % as shown in Table 5.9 This shows that regression model provides a good relationship between process and response parameters.

Table 5.9
Model summary for surface roughness

S	R-sq	R-sq(adj)	R-sq(pred)
0.425758	86.27%	78.03%	59.05%

5.5.5) Data Means Plot

The data means plot is shown in figure 5.2 is displaying effect of process parameters on response parameters.

Figure 5.2 Data means plot for surface roughness

5.6) Surface Roughness Analysis

The data means plot in Figure 5.2 shows the change of surface roughness related to other selected process parameters explained as under,

5.6.1) Traverse Speed (TS)

With the increase in traverse speed from 2mm/min to 6mm/min, the surface roughness raises. The quantity of particles impinging on a particular exposed surface reduces as the traverse speed increases, resulting in higher levels of surface roughness. Smooth cutting region (SCR) was reduced to 25% of total cutting surface at higher traverse speeds, compared to 60% at lower traverse speeds. Traverse speed is highly substantial factor for surface roughness [10] with a contribution of 57.54 % and the value of P is less than 0.05 as shown in Table 5.8. To obtain lowest surface roughness cutting at lower traverse speed should be opted.

5.6.2) Water Pressure (WP)

The change in surface roughness with the increase in the water pressure from 300MPa to 500MPa is negligible with respect to other process parameters. For surface roughness the contribution of water pressure is less than 1 % and is ranked 4 so it was pooled out during regression analysis.

5.6.3) Abrasive Flow Rate (AFR)

There is a negligible change over in surface roughness as abrasive flow changes from 200gm/ min to 250gm /min and then there is decrease in surface roughness with the increase in abrasive flow from 250gm/ min to 300gm/ min. With the increase in abrasive flow rate the amount of abrasive particles and available cutting edges per unit area of the exposed surface which will produce low surface roughness values. Abrasive flow rate is non-significant for surface roughness with P-value greater than 0.05 and contribution of 3.01 %.

5.6.4) Stand-off Distance (SOD)

Stand-off distance portrays a major role for surface roughness with P-value less than 0.05 with a contribution of 38.76 %. There is a minor change in surface roughness as stand-off distance changes from 2mm to 3mm and then surface roughness raises with the stand-off distance. Increase in stand-off distance will produce a wider jet diameter owing to external drag from neighbouring area resulting in reduced jet energy and higher values of surface roughness. Hence it is necessary to have a low stand-off distance for obtaining smooth surface.

5.7) Optimal Process Parameters

Thus, the optimal setting of Titanium Grade V for surface roughness is given in Table 5.10

Table 5.10
Optimal process parameters for surface roughness

Process Parameter	TS (mm/min)	WP (MPa)	AFR (gm/min)	SOD (mm)
Optimal Setting	2	400	300	3

5.8) Analysis for Abrasive Entrapment

5.8.1) XRD Analysis

To verify the entrapment of garnet, XRD of titanium alloy was done. The wavelength used was 1.54 Angstrom and source was Cu K. XRD pattern of titanium grade V, machined sample is shown in Figure 5.3. Presence of titanium was confirmed by reference # 44-1294. Additional peaks of silicon titanium and silicon were observed and confirmed by reference # 10-0225 and reference # 27-1402. This is the proof of entrapment of abrasive particles. XRD pattern has been zoomed as shown in Figure 5.4 to enhance the visibility of aluminium and silicon titanium peaks. The entrapment of abrasive particles in Titanium grade V was also confirmed by other researchers [17][16].

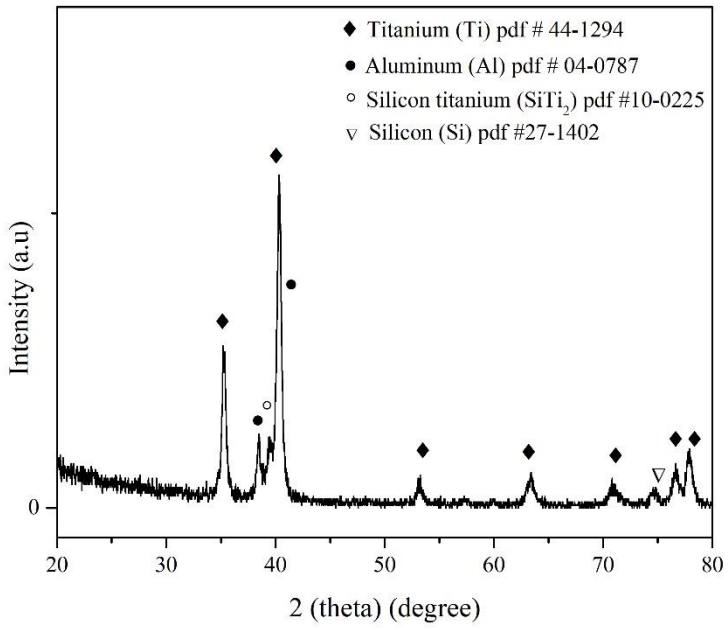

Figure 5.3 XRD pattern for Titanium grade V

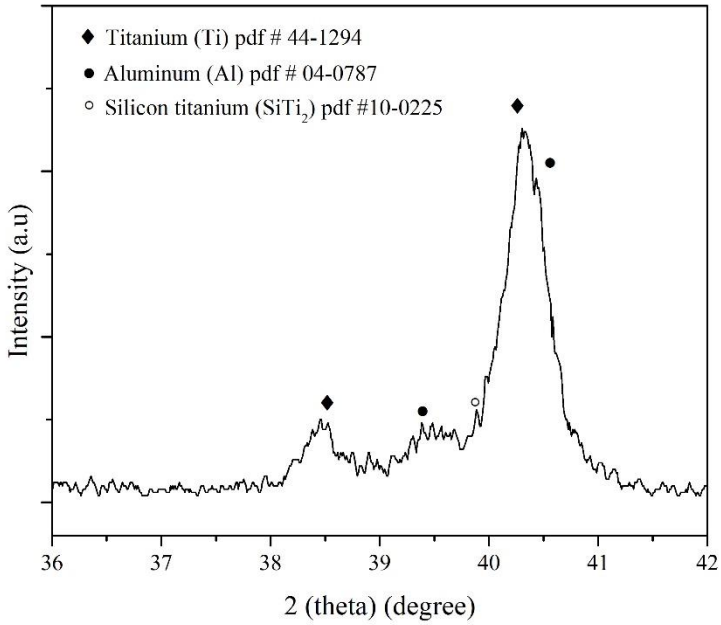

Figure 5.4 Zoomed XRD pattern for Titanium grade V

5.9) Grain Distortion Measurement

Selected machined samples were mounted, grinded and polished before conducting SEM analysis for measuring grain distortion. Grain distortion of machined samples is measured at three different points along the boundary line using ImageJ software shown in Table 5.11. Fig 5.5 shows the surfaces from the SEM backscatter detector at minimum and maximum traverse speed. The image shows a very trivial influence down to a few micrometres under the machined surface. An increase in grain distortion is observed from 9.44 µm to 14.87 µm as surface roughness is increased from 2.33 µm at to 4.84 µm respectively. Traverse speed was the most contributing factor for the surface roughness in case of titanium grade V. The average size of grain distortion and surface roughness increases as the traverse speed is raised, because a smaller quantity of abrasive particles will be contributing in cutting at higher traverse speed.

Table 5.11
Grain distortion of AWJ machined samples

S/No	Sample No	TS mm/min	WP MPa	AFR gm/min	SOD mm	Ra µm	Grain Distortion µm
1)	Ti(1)	2	300	200	2	2.33	9.44
2)	Ti(3)	2	500	300	4	3.02	10.56
3)	Ti(8)	6	400	200	4	4.84	14.87

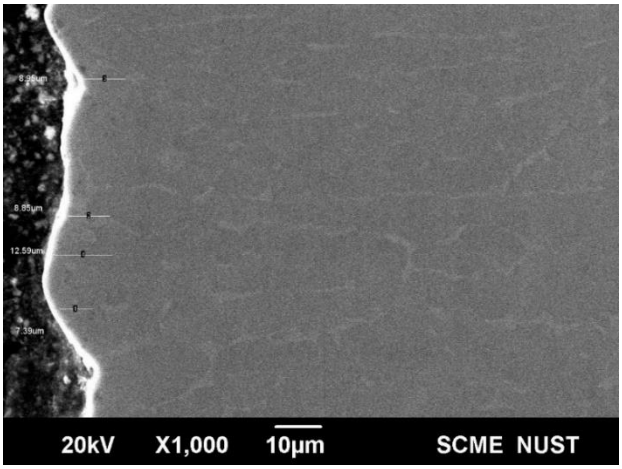

(a) Grain distortion of machined sample at min traverse speed

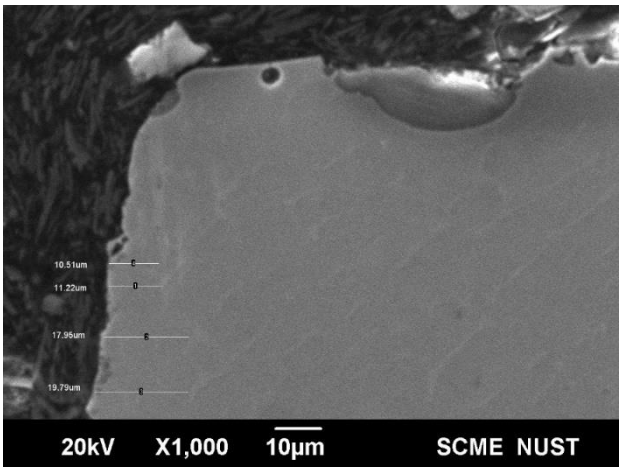

(b) Grain distortion of machined sample at max traverse speed

Figure No 5.5 Grain distortion of machined sample

5.10) Summary of Chapter

Kerf angle and surface roughness results for titanium grade V were tabulated. To discover major process parameters that affect the surface roughness and kerf angle, the Taguchi technique, together with variance analysis (ANOVA) were used which shows traverse speed as major factor for kerf angle and surface roughness. Regression equations are obtained for kerf angle. The plot for data displays the deviation of kerf angle and surface roughness in connection with other selected process parameters. The XRD analysis shows the entrapment of abrasive particles in machined samples. Scanning electron microscopy done for selected samples to measure the grain distortion, shows that lower values of traverse speed results in smaller values of grain distortion.

Chapter 6: “Conclusions”

6.1) Introduction

In this present work parametric analysis of Titanium grade V and Inconel 600 is done using AWJ cutting technique. Optimization of kerf angle and surface roughness is done using Taguchi methodology. Geometrical study of grain distortion is carried out using SEM analysis and for analysing entrapment of abrasive particles, XRD, SEM and EDS analysis are used.

Following conclusions have been drawn after analysis:

6.2) Conclusions for Inconel 600

- For kerf angle traverse speed and water pressure are most significant factors with contribution of 42.41% and 40.78 % respectively.
- Kerf angle can be minimized at lowest values of traverse speed and water pressure.
- Water pressure is the highly influential factor affecting surface roughness with contribution of 90.91 % while standoff distance is marked as sub significant.
- For obtaining smooth surface, lower values of water pressure and standoff distance should be preferred.
- AWJ cutting results in increased grain distortion with the increase in surface roughness and water pressure.
- Minimum grain distortion was obtained at lower water pressure at 300MPa, traverse speed at 2mm/min, abrasive flow rate 200gm/min and standoff distance 2mm.
- Abrasive particles were found to be entrapped in the machined surface after AWJ cutting.

6.3) Conclusions for Titanium Grade V

- For kerf taper angle traverse speed plays a major role with contribution of 85.2 %.
- Kerf taper angle can be minimized at lowest values of traverse speed at the cost of production rate.
- For surface roughness, traverse speed and standoff distance are most significant factors with contribution of 57.54 % and 38.74 % respectively.
- For obtaining smooth surface, lower level of traverse speed and standoff distance should be preferred.
- With the increase in traverse speed the grain distortion and surface roughness of the AWJ machined sample increases.
- Minimum grain distortion was obtained at lower value of traverse speed at 2mm/ min, water pressure 300MPa, abrasive flow rate 200 gm/min and standoff distance 2mm.
- Entrapment of abrasive particles is found in the AWJ machined samples.

6.4) Recommendations

- Optimization of grain distortion using Taguchi methodology to identify significant input parameters and their %age contribution.
- Effect of varying orifice diameter for obtaining maximum depth of cut for aerospace alloys.

References

[1] X. Liang, Z. Liu, and B. Wang, “State-of-the-art of surface integrity induced by tool wear effects in machining process of titanium and nickel alloys: A review,” *Meas. J. Int. Meas. Confed.*, vol. 132, pp. 150–181, 2019, doi: 10.1016/j.measurement.2018.09.045.

[2] S. H. I. Jaffery and P. T. Mativenga, “Wear mechanisms analysis for turning Ti-6Al-4V-towards the development of suitable tool coatings,” *Int. J. Adv. Manuf. Technol.*, vol. 58, no. 5–8, pp. 479–493, 2012, doi: 10.1007/s00170-011-3427-y.

[3] S. Saravanan, V. Vijayan, S. T. Jaya Suthahar, A. V. Balan, S. Sankar, and M. Ravichandran, “A review on recent progresses in machining methods based on abrasive water jet machining,” *Mater. Today Proc.*, vol. 21, no. xxxx, pp. 116–122, 2020, doi: 10.1016/j.matpr.2019.05.373.

[4] A. Perec, “Experimental research into alternative abrasive material for the abrasive water-jet cutting of titanium,” *Int. J. Adv. Manuf. Technol.*, vol. 97, no. 1–4, pp. 1529–1540, 2018, doi: 10.1007/s00170-018-1957-2.

[5] D. Krajcarz, “Comparison metal water jet cutting with laser and plasma cutting,” *Procedia Eng.*, vol. 69, pp. 838–843, 2014, doi: 10.1016/j.proeng.2014.03.061.

[6] M. Kantha Babu and O. V. Krishnaiah Chetty, “A study on recycling of abrasives in abrasive water jet machining,” *Wear*, vol. 254, no. 7–8, pp. 763–773, 2003, doi: 10.1016/S0043-1648(03)00256-4.

[7] A. Akkurt, “The effect of cutting process on surface microstructure and hardness of pure and Al 6061 aluminium alloy,” *Eng. Sci. Technol. an Int. J.*, vol. 18, no. 3, pp. 303–308, 2015, doi: 10.1016/j.jestch.2014.07.004.

[8] J. Holmberg, J. Berglund, A. Wretland, and T. Beno, “Evaluation of surface

integrity after high energy machining with EDM, laser beam machining and abrasive water jet machining of alloy 718," *Int. J. Adv. Manuf. Technol.*, vol. 100, no. 5–8, pp. 1575–1591, 2019, doi: 10.1007/s00170-018-2697-z.

[9] J. J. R. Jegaraj and N. R. Babu, "A strategy for efficient and quality cutting of materials with abrasive waterjets considering the variation in orifice and focusing nozzle diameter," *Int. J. Mach. Tools Manuf.*, vol. 45, no. 12–13, pp. 1443–1450, 2005, doi: 10.1016/j.ijmachtools.2005.01.020.

[10] A. Hascalik, U. Çaydaş, and H. Gürün, "Effect of traverse speed on abrasive waterjet machining of Ti-6Al-4V alloy," *Mater. Des.*, vol. 28, no. 6, pp. 1953–1957, 2007, doi: 10.1016/j.matdes.2006.04.020.

[11] M. C. Patel, S. B. Patel, and R. H. Patel, "Parametric analysis of abrasive water jet machining of aluminium 6351 t6," *Int. J. Technol. Res. Eng.*, vol. 1, no. 12, pp. 1458–1467, 2014.

[12] P. Shanmughasundaram, "Influence of abrasive water jet machining parameters on the surface roughness of eutectic Al-SI alloy-graphite composites," *Mater. Phys. Mech.*, vol. 19, no. 1, pp. 1–8, 2014.

[13] D. S. Reddy, A. S. Kumar, and M. S. Rao, "Parametric Optimization of Abrasive Water Jet Machining of Inconel 800H Using Taguchi Methodology," *Univers. J. Mech. Eng.*, vol. 2, no. 5, pp. 158–162, 2014, doi: 10.13189/ujme.2014.020502.

[14] R. Shukla and D. Singh, *Experimentation investigation of abrasive water jet machining parameters using Taguchi and Evolutionary optimization techniques*, vol. 32. Elsevier, 2017.

[15] K. S. K. Sasikumar, K. P. Arulshri, K. Ponappa, and M. Uthayakumar, "A study on kerf characteristics of hybrid aluminium 7075 metal matrix composites machined using abrasive water jet machining technology," *Proc. Inst. Mech. Eng. Part B J. Eng. Manuf.*, vol. 232, no. 4, pp. 690–704, 2018, doi: 10.1177/0954405416654085.

[16] P. R. Thakre, R. P. Singh, and G. Slipher, *Mechanics of Composite , Hybrid and Multifunctional Materials , Volume 5*, vol. 5. 2018.

[17] Y. W. Seo, M. Ramulu, and D. Kim, "Machinability of titanium alloy (Ti-6Al-4V) by abrasive waterjets," *Proc. Inst. Mech. Eng. Part B J. Eng. Manuf.*, vol. 217, no. 12, pp. 1709–1721, 2003, doi: 10.1243/095440503772680631.

[18] A. Gnanavelbabu, P. Saravanan, K. Rajkumar, and S. Karthikeyan, "Experimental Investigations on Multiple Responses in Abrasive Waterjet Machining of Ti-6Al-4V Alloy," *Mater. Today Proc.*, vol. 5, no. 5, pp. 13413–13421, 2018, doi: 10.1016/j.matpr.2018.02.335.

[19] A. Henning, M. Lo, E. Schubert, and P. Miles, *Effect of Particle Fragmentation on Cutting Performance in Abrasive Waterjets*. 2021.

[20] M. Uthayakumar, M. A. Khan, S. T. Kumaran, A. Slota, and J. Zajac, "Machinability of Nickel-Based Superalloy by Abrasive Water Jet Machining," *Mater. Manuf. Process.*, vol. 31, no. 13, pp. 1733–1739, 2016, doi: 10.1080/10426914.2015.1103859.

[21] M. Adam Khan and K. Gupta, "Machining Ni-Cr-Fe based superalloy using abrasive water jet cutting process and its surface studies," *Mater. Today Proc.*, vol. 19, no. xxxx, pp. 2139–2143, 2019, doi: 10.1016/j.matpr.2019.07.227.

[22] I. Karakurt, G. Aydin, and K. Aydiner, "An experimental study on the depth of cut of granite in abrasive waterjet cutting," *Mater. Manuf. Process.*, vol. 27, no. 5, pp. 538–544, 2012, doi: 10.1080/10426914.2011.593231.

[23] M. Ay, U. Çaydaş, and A. Hasçalik, "Effect of traverse speed on abrasive waterjet machining of age hardened inconel 718 nickel-based superalloy," *Mater. Manuf. Process.*, vol. 25, no. 10, pp. 1160–1165, 2010, doi: 10.1080/10426914.2010.502953.

[24] V. Gupta, P. M. Pandey, M. P. Garg, R. Khanna, and N. K. Batra, "Minimization of Kerf Taper Angle and Kerf Width Using Taguchi's Method in Abrasive Water

Jet Machining of Marble," *Procedia Mater. Sci.*, vol. 6, no. Icmpc, pp. 140–149, 2014, doi: 10.1016/j.mspro.2014.07.017.

[25] X. Sourd, R. Zitoune, A. Hejjaji, M. Salem, A. Hor, and D. Lamouche, "Plain water jet cleaning of titanium alloy after abrasive water jet milling: Surface contamination and quality analysis in the context of maintenance," *Wear*, vol. 477, no. September 2020, p. 203833, 2021, doi: 10.1016/j.wear.2021.203833.

[26] F. Boud, J. W. Murray, L. F. Loo, A. T. Clare, and P. K. Kinnell, "Soluble abrasives for waterjet machining," *Mater. Manuf. Process.*, vol. 29, no. 11–12, pp. 1346–1352, 2014, doi: 10.1080/10426914.2014.930949.

[27] G. Fowler, P. H. Shipway, and I. R. Pashby, "A technical note on grit embedment following abrasive water-jet milling of a titanium alloy," *J. Mater. Process. Technol.*, vol. 159, no. 3, pp. 356–368, 2005, doi: 10.1016/j.jmatprotec.2004.05.024.

CERTIFICATE OF COMPLETENESS

It is hereby certified that the dissertation submitted by **NS Lubna Sharif**, Reg No. **00000204365** Titled: ***Parametric Investigation of Thick Metallic Section (Aerospace Alloys) Cutting by Abrasive Water Jet*** *has* been checked/reviewed and its contents are complete in all respects.

Supervisor's Name: **Dr. Khalid Mahmood** Signature: _____

Date: _____